Environmental Science and Pollution Research
https://doi.org/10.1007/s11356-023-25958-x

CHALLENGES IN MANAGING GROUNDWATER RESOURCES AND HUMAN HEALTH RISK ASSESSMENT OF EMERGING GROUNDWATER CONTAMINATIONS

Groundwater fluoride and nitrate contamination and associated human health risk assessment in South Punjab, Pakistan

Javed Iqbal[1,2] · Chunli Su[1,2] · Mengzhu Wang[1,2] · Hasnain Abbas[1] · Muhammad Yousuf Jat Baloch[3] · Junaid Ghani[4] · Zahid Ullah[1] · Md. Enamul Huq[5]

Received: 9 November 2022 / Accepted: 11 February 2023

Abstract

Consumption of high fluoride (F^-) and nitrate (NO_3^-) containing water may pose serious health hazards. One hundred sixty-one groundwater samples were collected from drinking wells in Khushab district, Punjab Province, Pakistan, to determine the causes of elevated F^- and NO_3^- concentrations, and to estimate the human health risks posed by groundwater contamination. The results showed pH of the groundwater samples ranged from slightly neutral to alkaline, and Na^+ and HCO_3^- ions dominated the groundwater. Piper diagram and bivariate plots indicated that the key factors regulating groundwater hydrochemistry were weathering of silicates, dissolution of evaporates, evaporation, cation exchange, and anthropogenic activities. The F^- content of groundwater ranged from 0.06 to 7.9 mg/L, and 25.46% of groundwater samples contained high-level fluoride concentration ($F^- > 1.5$ mg/L), which exceeds the (WHO Guidelines for drinking-water quality: incorporating the first and second addenda, WHO, Geneva, 2022) guidelines of drinking-water quality. Inverse geochemical modeling indicates that weathering and dissolution of fluoride-rich minerals were the primary causes of F^- in groundwater. High F^- can be attributed to low concentration of calcium-containing minerals along the flow path. The concentrations of NO_3^- in groundwater varied from 0.1 to 70 mg/L; some samples are slightly exceeding the (WHO Guidelines for drinking-water quality: incorporating the first and second addenda, WHO, Geneva, 2022) guidelines for drinking-water quality. Elevated NO_3^- content was attributed to the anthropogenic activities revealed by PCA analysis. The high levels of nitrates found in the study region are a result of various human-caused factors, including leaks from septic systems, the use of nitrogen-rich fertilizers, and waste from households, farming operations, and livestock. The hazard quotient (HQ) and total hazard index (THI) of F^- and NO_3^- showed high non-carcinogenic risk (> 1) via groundwater consumption, demonstrating a high potential risk to the local population. This study is significant because it is the most comprehensive examination of water quality, groundwater hydrogeochemistry, and health risk assessment in the Khushab district to date, and it will serve as a baseline for future studies. Some sustainable measures are urgent to reduce the F^- and NO_3^- content in the groundwater.

Keywords Nitrate · Fluoride · Groundwater quality · Water–rock interaction

Introduction

Groundwater is an essential source of fresh water in arid and semi-arid regions worldwide, but different pathogens and chemical contamination frequently challenge water

Responsible Editor: Xianliang Yi

✉ Chunli Su
chl.su@cug.edu.cn

[1] School of Environmental Studies, China University of Geosciences, Wuhan 430074, China

[2] State Environmental Protection Key Laboratory of Source Apportionment and Control of Aquatic Pollution, China University of Geosciences, Wuhan 430074, China

[3] College of New Energy and Environment, Jilin University, Changchun 130021, China

[4] Department of Biological, Geological, and Environmental Sciences, Alma Mater Studiorum University of Bologna, 40126 Bologna, Italy

[5] College of Environment, Hohai University, Nanjing, China

Published online: 22 February 2023

safety (Jat Baloch et al. 2022a; Zhang et al. 2022a, b). Almost 2.5 billion people depend heavily on groundwater for their daily needs, particularly for drinking (Ghani et al. 2022; Huq et al. 2020; McDonald et al. 2011; Rashid et al. 2018). Groundwater demand is increasing daily due to population growth and the lack of alternative water sources for various utilities (Sajjad et al. 2022; Tariq et al. 2022). Due to environmental changes and human activities, groundwater quality is drastically declining, which directly affects human health and causes serious problems (Dilpazeer et al. 2023; Jat Baloch et al. 2022b; Kamruzzaman et al. 2020; Zhang et al. 2018). Human use of high levels of F^- and NO_3^- containing groundwater has been linked to non-carcinogenic concerns worldwide (Qasemi et al. 2019; Rao et al. 2021; Tran et al. 2021). Long-term ingesting of polluted groundwater (inorganic or organic) may endanger the local population's health (Baloch et al. 2020; Su et al. 2016, 2021).

For the past two decades, contamination of groundwater by F^- and NO_3^- has been a significant public health concern (Qasemi et al. 2023). Many studies on the groundwater quality related to elevated F^- have been conducted in arid and semi-arid regions around the world (Alam and Ahmad 2014; Khattak et al. 2022; Lanjwani et al. 2022; Mwiathi et al. 2022; Su et al. 2013, 2015). The World Health Organization (WHO 2022) recommends a permissible level of 1.5 mg/L of F^- in groundwater for human consumption. Prolonged consumption of geogenic pollutants, such as F^-, can lead to fluorosis (a condition affecting the teeth and bones), characterized by symptoms such as stiffness, osteoporosis, calcification of ligaments, limps, and arthritis (Aurrecoechea et al. 2009; Qasemi et al. 2022; Rao et al. 2022b; Subba Rao et al. 2020). Fluorosis is a highly prevalent condition, affecting 260 million people in 25 countries around the world, with 100 million of them in Southeast Asia, including India, Pakistan, and Sri Lanka (Mridha et al. 2021; Rasool et al. 2018). Human health has been linked to elevated NO_3^- levels in drinking water (Rao et al. 2022b; Ward et al. 2018). Due to the risk of infant methemoglobinemia, the US Environmental Protection Agency established a maximum contaminant limit (MCL) of 10 mg/L for NO_3^- (Beaver et al. 2014). Exceedances of the NO_3^- MCL is excessive in water. Epidemiological studies have linked NO_3^- in drinking water to colorectal cancer, childhood central nervous system tumors, thyroid disorders, and neural tube defects at levels above the MCL (Gugulothu et al. 2022a; Ransom et al. 2022).

F^- is found in groundwater due to anthropogenic sources and rock weathering (Brindha and Elango 2011; Talpur et al. 2020). During weathering, the fluoride-bearing minerals (e.g., amphiboles, apatite, biotite fluorite, muscovite), release F^- into the groundwater. Temperature, pH, calcium and bicarbonate ion concentration in water, and other factors have all impacted the availability and solubility of fluorine-bearing minerals. In contrast to the anthropogenic degradation of surface water, geogenic pollution of groundwater is difficult to detect and manage (Iqbal et al. 2021; Nabizadehb et al. 2019; Rezaei et al. 2017). Phosphate fertilizers, herbicides, sewage and sludge, and other agricultural practices have all been linked to increased F^- concentrations in groundwater (Baloch and Mangi 2019, Iqbal et al. 2021, Kundu and Mandal 2009, Talpur et al. 2020). The main mechanisms that result in F^- enrichment in groundwater are dissolution and precipitation (Sahin et al. 2021), adsorption/desorption (Zhang and Selim 2005), ion exchange (Nagendra Rao 2003), evaporation (Adimalla et al. 2018), mixing (Sakram et al. 2019), and anthropogenic activities (Haji et al. 2021). The increased NO_3^- concentrations caused by industrial and agricultural activities may impact groundwater quality (Liu et al. 2021). Anthropogenic and natural activities, such as nitrogen fertilizers, can transfer NO_3^- into groundwater (Shukla and Saxena 2018). Chemical fertilizers, atmospheric precipitation, soil organic nitrogen, manure, and sewage are all potential sources of NO_3^- (Inyang et al. 2012). A thorough understanding of hydrogeochemical properties and contamination status is required to protect groundwater resources in Pakistan and ensure drinking water safety (Talib et al. 2019; Ullah et al. 2022).

In semi-arid and arid areas of Pakistan, groundwater is the most essential source of domestic water (Abbas et al. 2018; Jat Baloch et al. 2021a). According to the Pakistan Council of Research in Water Resources (PCRWR), polluted groundwater is the leading cause of diseases in Pakistan (Al-Rasheed 2013). Numerous studies on F^- and NO_3^- contamination of groundwater in Pakistan have been conducted in recent years (Anjum et al. 2013; Farooqi et al. 2007; Masood et al. 2022; Rafique et al. 2009; Raza et al. 2016; Tahir and Rasheed 2008). Contamination of groundwater sources by F^- in Pakistan has been reported in various regions, including Dargai (Rashid et al. 2020), Negar Parkar (Rafique et al. 2009), Sialkot (Ullah et al. 2009), UmarKot (Rafique et al. 2015), Swat (Rashid et al. 2018), and Peshawar (Ahmad et al. 2020). In twenty-one cities of Pakistan, the NO_3^- concentrations in groundwater were higher than the WHO 2022 recommended drinking water quality limits (Gelfand et al. 2011; Rehman et al. 2020; Tahir and Rasheed 2008). Twenty-five percent of the groundwater of Rawalpindi, Pakistan, is nitrate-polluted (Khan et al. 2005; Soomro et al. 2017). To date, there has been a lack of research on the hydrogeochemistry of groundwater and its potential health impacts in the Khushab district. Therefore, a comprehensive study on the hydrogeochemical characteristics and potential health risks of groundwater for the local population is needed to be conducted. The objectives of this study were (1) to identify the geochemical processes that cause F^- and NO_3^- enrichment in groundwater, and (2) to assess

the potential health risks of exposure to F^- and NO_3^- in the groundwater.

Materials and methods

Study area

Khushab district is located in Punjab Province, Pakistan, at 32°01′7.57″ N and 72°12′16.21″ E. It covers a total area of

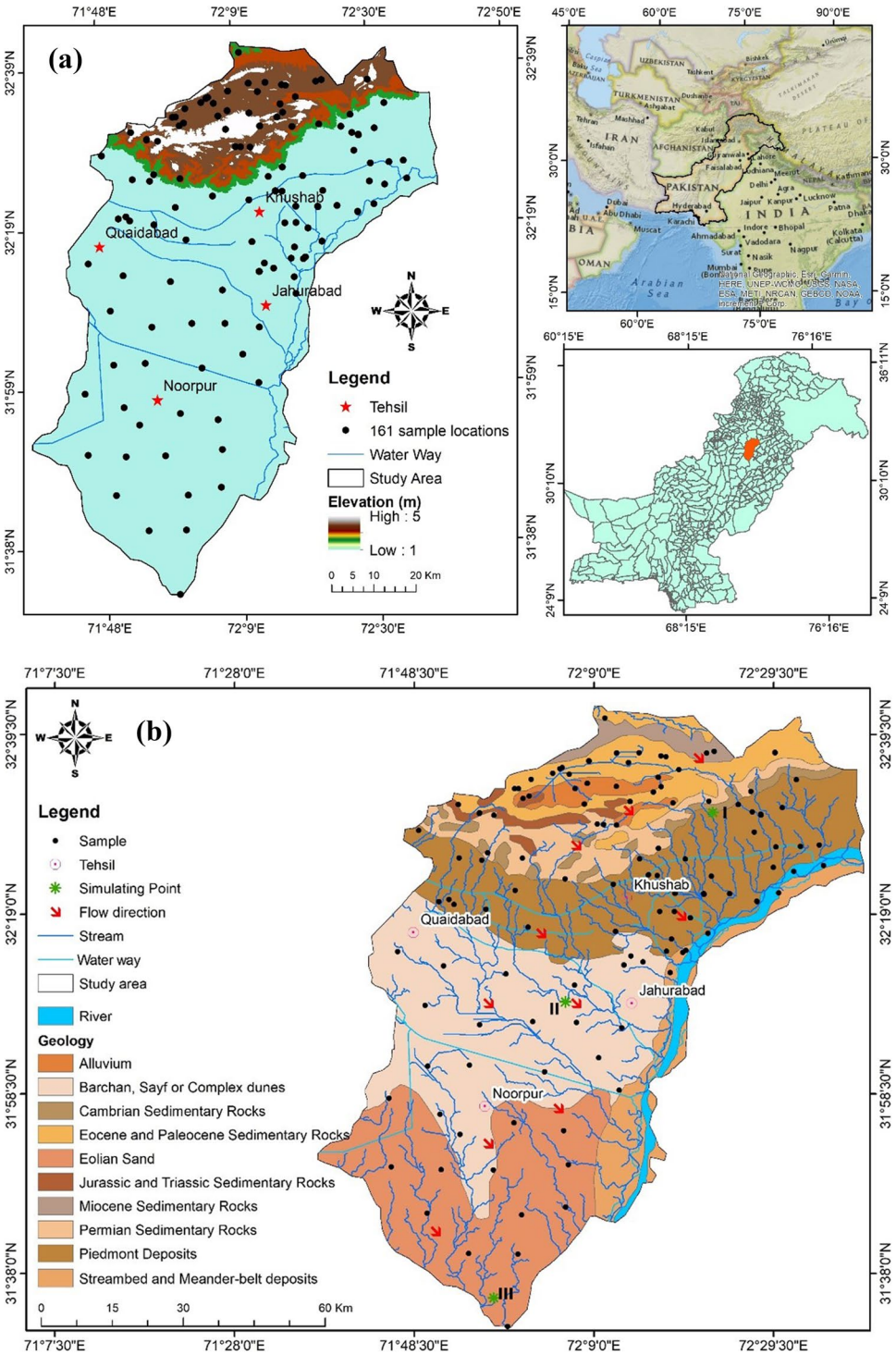

Fig. 1 Location and sampling sites (**a**), and hydrogeology map (**b**) of the study area

6511 km^2. The population was 905,711 at the 2017 census, with 24.76% living in urban areas (Fig. 1). The district comprises four tehsils, namely, Khushab, Quaidabad, Nurpur, and Jahurabad. The air temperatures in the summer range from 35 to 46 °C, while temperatures in the winter vary from 6 to 13 °C, with annual precipitation ranging from 150 to 350 mm (Chaudhari et al. 2014).

Khushab is situated in the Salt Range foothills, composed of heavily fractured and deformed rocks containing fossils from the Precambrian to the Pleistocene. The study area is one of the parts of the Indus plains through which the Indus River and its tributaries drain. A doab is a flat area in the Indus plain that means "a place surrounded by two rivers" (Puri et al. 2009). The five doabs of the Indus plains are Rechna Doab, Thal Doab, Bari Doab, Chaj Doab, and Bist Doab. The Jhelum River runs through the research area in Thal Doab's north-eastern region, separating the Sargodha district tehsils of Khushab and Shahpur.

Unconsolidated but extremely permeable alluvium deposits can be found up to a depth of more than 300 m throughout the research area (Swarzenski 1965). In addition, the Indus plain contains discontinuous, low-permeability material. As a result, sand accounts for nearly 70% of alluvium and serves as a highly transmissive and unconfined aquifers (Cheema and Bastiaanssen 2010; Hussain et al. 2017). The research area's permeability coefficients range from 0.05 to 1.2 m/s (Greenman et al. 1967). Khushab comprises massive yet unconsolidated Quaternary alluvial and eolian deposits on top of Precambrian basement rocks. Alluvium deposits contain fine to medium sand, clay, and silt. Coarser concentrated sediments can be found at a depth of 180 m near Quaid Abad and Bundiyal. The floodplains of the Jhelum River are covered in heavy sand deposits with a small amount of gravel. Thin silt and clay lenses with limited vertical and lateral extension are found in sand deposits (Akram 2014). The Jhelum River recharges aquifers through its bed and is responsible for flooding on flood plains. Rainwater is another critical source of aquifer recharge in the study region.

Sampling and analysis

To assess the quality of groundwater in the Khushab district, 161 samples were collected from shallow aquifers (< 35 m) between June and August 2020. The samples were then filtered through a 0.45-µm filter for further analysis. The American Public Health Association's standard methods were followed (APHA et al. 2005) (Jat Baloch et al. 2022b). The samples were then stored in 120-mL glass bottles that had been thoroughly rinsed and washed. These groundwater samples were then tested in the Pakistan Council of Research in Water Resources (PCRWR) water quality laboratory. The pH, electrical conductivity (EC), total dissolved solids (TDS), total hardness (TH), and turbidity were evaluated in the study area using the multiparameter analyzer (Hanna HI9829). The samples were examined for significant anions, such as NO_3^-, SO_4^{2-}, and PO_4^{3-}, using a UV–VIS spectrophotometer (Germany). The concentration of F^- was determined using "Mohr's method and fluoride analyzer" ISE (ion-selective electrode) (Rashid et al. 2018). Bicarbonate (HCO_3^-) and chloride (Cl^-) were determined using titration. Calcium (Ca^{2+}) and magnesium (Mg^{2+}) concentrations were measured by volumetric titration with ethylene diamine tetra acetic acid. The flame photometer was used to measure sodium (Na^+) and potassium (K^+) concentrations (Zhou et al. 2021). Arsenic (As) was determined in the samples using atomic absorption spectrophotometer (AAS Vario 6, Analytik Jena, Jena, Germany) (Baloch et al. 2022). To check the accuracy of the results, the charge balance error (CBE) for each sample was calculated using Eq. (1) (ionic concentrations are measured in meq/L). Groundwater samples containing ± 5% CBE were chosen for further analysis (Jat Baloch et al. 2022a).

$$\mathrm{CBE} = \frac{[\Sigma\text{cations} - \Sigma\text{anions}]}{[\Sigma\text{cations} + \Sigma\text{anions}]} \times 100 \quad (1)$$

Health risk assessment

The F^- and NO_3^- and have been chosen to assess the risk to human health. Estimating the average daily dosage for adults and children (ADD) used the oral intake procedure (Gugulothu et al. 2022a; Li and Wu 2019; Selvam et al. 2020; Subba Rao 2021). The average daily dosage (ADD), hazard quotient (HQ), and total health index (THI) were computed using Eqs. 2, 3, and 4 (USEPA 2005).

$$\mathrm{ADD} = \frac{\mathrm{CPW} \times \mathrm{IR} \times \mathrm{Ed} \times \mathrm{EF}}{\mathrm{ABW} \times \mathrm{AET}} \quad (2)$$

ADD denotes F^- and NO_3^- and ingestion (mg/kg/day), CPW denotes the specific groundwater pollutant (mg/L), and the ingestion rate is signified by IR, which is 2.5 L/day for adults and 0.78 L/day for children (Narsimha and Rajitha 2018). The ED stands for exposure duration (64 years for adults, 12 years for children, and 1 year for infants) (Ahada and Suthar 2019). An adult's average body weight (ABW) is 57.5 kg, while children's ABW is 18.7 kg, and infants' ABW is 16.9 kg; adults have an average exposure time (AET) of 23,360 days, children have an AET of 4380 days, and the AET of 365 days for infants.

$$HQ = \frac{ADD}{RfD} \quad (3)$$

$$\text{Total Hazard Index(THI)} = \Sigma HQ \quad (4)$$

where HQ stands for hazards quotient and RfD also known as the F^- and NO_3^- and exposure dosages of 0.06 and 1.6 mg/kg/day, respectively. The THI was used to estimate the health risk posed by the ingestion exposure pathway. THI ≤ 1 values are considered to indicate no significant non-carcinogenic risk. THI > 1 values are defined to indicate the occurrence of non-carcinogenic risk in the exposed population.

Numerical methods

Statistical analysis helps in the interpretation of data sets by identifying various acts (Rahman et al. 2022; Ravindra et al. 2022; Xue-Jie et al. 2013). Hydrochemical processes were described using the statistical multivariate analysis method, which involved decreasing the amount of information and grouping the data (Uddin et al. 2018). The principal component analysis is a multivariate approach for reducing many connected variables into a manageable number of unrelated variables. It is based on covariance, which shows how groundwater variables interact with each other (Purushotham et al. 2011). This technique extensively extracts valuable information from groundwater hydrochemical datasets (Singh et al. 2020). Principal components were extracted using the varimax rotation Kaiser normalization method (PCs). The PCA was calculated using XLSTAT 2022.

The spatial maps were created using the IDW interpolation method. ArcGIS 10.3 was used to create maps of geographic location and spatial distribution. The hydrochemistry software PHREEQC 3.4 was used to calculate the saturation indices of minerals and geochemical inverse modeling.

Results

Groundwater chemistry and spatial distribution

Statistical summaries of the measured physicochemical parameters for the groundwater samples are depicted in Table 1 and compared to the WHO 2022 guideline limits for drinking water (WHO 2022). The pH of the groundwater varied from 6.7 to 8.5, with a mean of 7.7. The turbidity levels ranged from 0.3 to 4600 NTU, with a mean of 23.85 NTU. The EC is a measurement of the capability of water to transmit an electric current between dissolved salts, which ranges from 200 to 14,120 µS/cm. The hydrochemical analysis showed that TDS concentration ranged from 112 to 8051 mg/L, with a mean of 1070 mg/L. The total hardness varied between 90 and 4600 mg/L, with an average of 457.7 mg/L.

Major cation abundance was found to be in the following order: $Na^+ > Ca^{2+} > Mg^{2+} > K^+$. Na^+ is the dominating cation in the study region, ranging from

Table 1 Statistical physicochemical parameters of groundwater samples ($n = 161$) collected from the Khanewal district

Parameters	Minimum	Maximum	Mean	Standard deviation	WHO (2022) standard
pH	6.77	8.55	7.72	0.3464	6.5–8.5
EC (µS/cm)	200	14,120	1849	2114	1000
TDS (mg/L)	112	8051	1070	1197	1000
Turbidity	0.3	4600	457.7	440.9	5
TH (mg/L)	90	530	215.7	97.13	300
Na^+ (mg/L)	5.0	2460	208.6	315.1	200
Mg^{2+} (mg/L)	5.0	513	54.6	54.77	150
K^+ (mg/L)	1.0	440	11.3	40.5	12
F^- (mg/L)	0.06	7.9	1.06	0.9315	1.5
Ca^{2+} (mg/L)	10	992	92.7	94.49	200
Fe^{2+} (mg/L)	0.01	1.21	0.11	0.1897	0.3
PO_4^{3-} (mg/L)	0.01	0.13	0.04	0.0304	0.1
Cl^- (mg/L)	10	3212	263.7	502.1	250
SO_4^{2-} (mg/L)	15	2100	254.7	312.5	250
NO_3^- (mg/L)	0.1	70	8.88	14.31	50
HCO_3^- (mg/L)	83	817	309.3	126.7	250
As (µg/L)	5	15	2.73	4.03	10

5.00 to 2460 mg/L, with an average of 440.0 mg/L. Ca^{2+} concentrations vary from 10.0 to 992.0 mg/L, with a mean of 99.2 mg/L. In the study region, anions are abundant in the following order: $HCO_3^- > Cl^- > SO_4^{2-} > F^- > PO_4^{3-}$. HCO_3^- concentrations ranged from 83.0 to 817 mg/L, with a mean of 309.3 mg/L, making it the most prevalent anion in groundwater. Cl^- concentrations are from 10.0 to 3212 mg/L, with a mean of 263.7 mg/L. The concentrations of SO_4^{2-} and PO_4^{3-} varied from 15.0 to 2100 mg/L and 0.01–0.13 mg/L, with a mean of 254.74 mg/L and 0.04 mg/L, accordingly. The average NO_3^- content in groundwater was 8.89 mg/L, ranging from 0.1 to 70 mg/L. In 23.60% of groundwater samples, the NO_3^- concentration exceeded the WHO 2022 permissible 10 mg/L limits.

The F^- concentration ranged from 0.06 to 7.9 mg/L, with a mean of 1.06 mg/L. According to WHO guidelines, F^- concentrations in 25.46% of the groundwater samples surpassed the allowable limit of 1.5 mg/L for drinking purposes (WHO 2022). High F^- groundwater occurred widespread in the study region. High F^- groundwater concentrations were found primarily in the southeastern and the sporadic parts in the north of the study area (Fig. 3). Hydrogeochemical faces of the groundwater varied greatly, from fresh HCO_3-Ca to saline Cl-Na, mixed HCO_3-Na-Ca and mixed Cl-Mg-Ca type and followed by HCO_3-Ca, HCO_3-Na, and Cl-Ca type (Fig. 2). The hydrochemical faces of high F^- groundwaters are categorized as HCO_3^- type and Na^+ type as shown in the Piper diagram (Fig. 2). Furthermore, groundwaters with elevated F^- contained elevated Na^+ and HCO_3^-. This is in accordance with the hydrogeochemical characteristics of high-fluoride groundwater reported in other regions (Chen et al. 2020; Li et al. 2019).

Spatial distribution of hydrochemical components

The spatial distribution of groundwater physicochemical analysis reveals an anomalous groundwater quality zone (Rao et al. 2022c) (Fig. 3). The concentration of TDS in groundwater exceeds its permissible limit for drinking in 38.5% of the study area. The greater the value, the higher the quantity of salt leaching, sewage infiltration, and the effect of nearby saline sources in our study region (Khan et al. 2018). The central part of the study area had elevated Na^+ concentrations. In contrast, Mg^{2+} and Ca^{2+} concentrations were relatively low in the study area except for a few sporadic sampling points (Fig. 3). Groundwater alkalinity is caused by HCO_3^- (Adams et al. 2001). The groundwater quality in a large portion of the study area is alkaline, indicating that the dissolved carbonates are mostly bicarbonates. Cl^- levels are slightly elevated in a larger patch, particularly in central and western regions of the study area, which pose a health risk. This is due to poor fluxing and the presence of the mineral halite. It is worth noting that SO_4^{2-} content was significantly higher in the study area, particularly in the central and northwestern

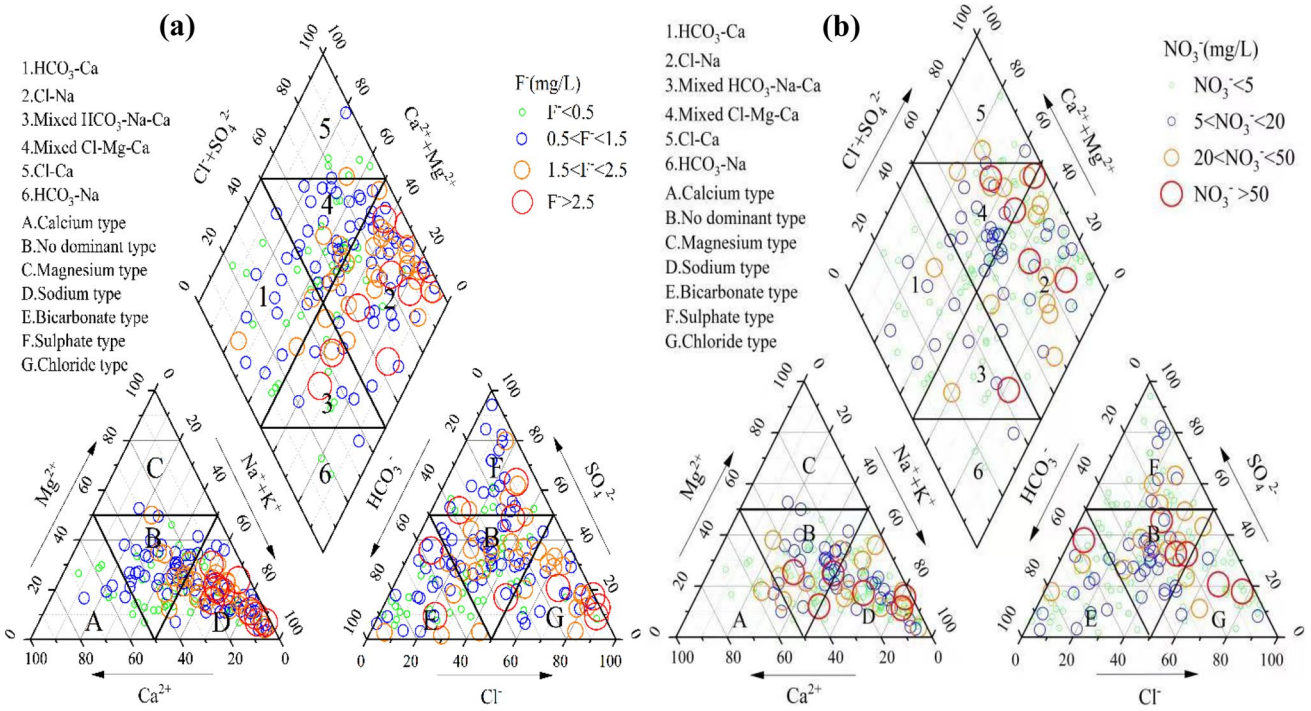

Fig. 2 Geochemical evolution of groundwater types with fluoride (**a**) and nitrate (**b**) concentrations indicated as bubbles

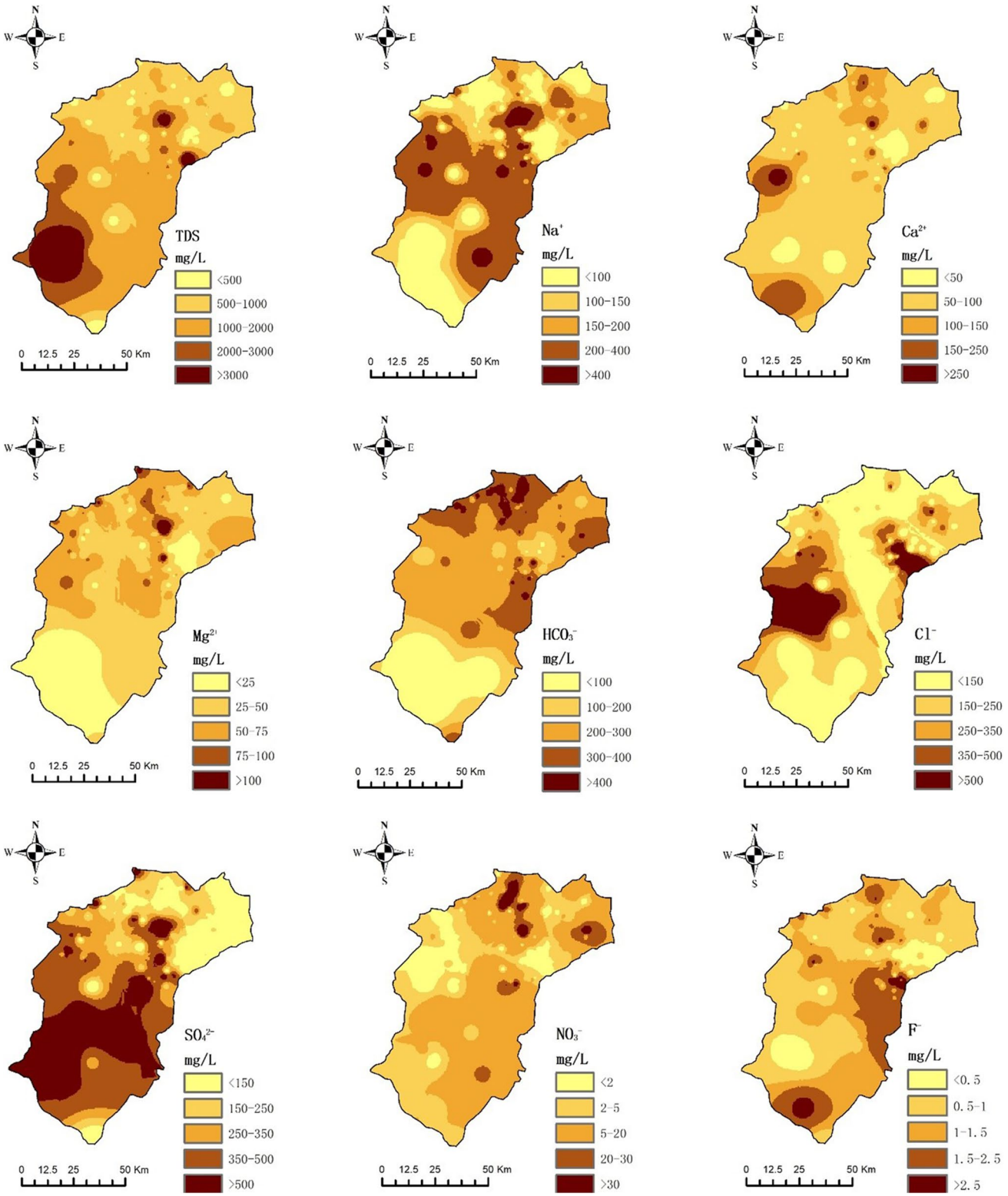

Fig. 3 Spatial distribution pattern of TDS (mg/L), Na^+ (mg/L), Ca^{2+} (mg/L), Mg^{2+} (mg/L), HCO_3^- (mg/L), Cl^- (mg/L), SO_4^{2-} (mg/L), NO_3^- (mg/L), and $F.^-$ (mg/L)

regions. Mineral dissolution, atmospheric deposition, and other anthropogenic sources contribute to groundwater sulfate. High NO_3^- levels in the groundwater were found in the central and northern portions of the study region, as shown in the spatial distribution map, which is due to domestic waste and agricultural activities.

Table 2 Principal component analysis of selected groundwater parameters for Khushab district

Parameters	PC1	PC2	PC3	PC4
pH	−0.33	**0.63**	0.11	−0.28
EC	**0.97**	0.17	0.08	0.02
TDS	**0.98**	0.17	0.07	0.01
Turbidity	−0.03	−0.20	**0.70**	−0.15
Hardness	**0.90**	−0.29	−0.01	0.11
F^-	0.47	**0.51**	−0.22	−0.35
Cl^-	**0.90**	0.22	0.18	0.14
NO_3^-	0.40	−0.50	−0.27	−0.23
HCO_3^-	0.28	−0.20	−0.52	−0.39
SO_4^{2-}	**0.91**	0.12	0.06	−0.04
PO_4^{3-}	0.01	0.11	−0.11	**0.70**
Ca^{2+}	**0.80**	−0.42	−0.01	0.15
Mg^{2+}	**0.93**	−0.13	−0.02	0.05
Na^+	**0.83**	0.43	0.12	−0.02
K^+	0.37	−0.13	−0.10	−0.31
Fe^{2+}	0.00	−0.26	**0.54**	−0.45
As	−0.05	0.12	−0.40	−0.17
Eigenvalues	7.24	1.68	1.43	1.30
Variance (%)	42.61	9.91	8.43	7.66
Cumulative (%)	42.61	52.52	60.94	68.60

Bold values are the main contributors to PCA

Discussion

Source appointment by principal component analysis (PCA)

The PCA can be used to determine the critical ion sources and geochemical processes that influence groundwater quality (Herczeg et al. 2001). A factor loading value of one or more shows a strong correlation between the factors and the variables. In contrast, values greater than 0.5 are considered significant. The four principal components account for 68.60% of the total variance for log-transformed data. PC1 has the highest data variance, followed by PC2, PC3, and PC4 (Table 2 and Fig. 4). PC1 had strong positive loadings, particularly for EC, TDS, hardness, Cl^-, SO_4^{2-}, Ca^{2+}, Mg^{2+}, and Na^+, which explained 42.61% of the total variance. PC1 is mainly made up of essential cations and anions from anthropogenic and natural sources. Mineral weathering and water–rock interaction are two natural processes in the aquifer (Rashid et al. 2022), and anthropogenic sources include domestic sewage in the study. This factor identifies agricultural activities as the other contributing process due to NO_3^-, Mg^{2+}, and SO_4^{2-}. The PC2 accounts for 9.91% and consisting high positive loadings of pH and F^-, indicating that pH controls F^- in groundwater. Fluoride minerals cause elevated F^- concentration in the study area. The PC3, which accounts for 8.43% of the total variance, indicates a high positive loading turbidity and Fe^{2+}. Poorly designed and shallowly constructed wells contribute to turbidity (Azis 2015; Jat Baloch et al. 2021b), and higher Fe^{2+} concentrations in groundwater are caused by ferruginous minerals on the surface of the earth (Raju 2006). With a total variance of 7.66%, PC4 shows moderate loadings

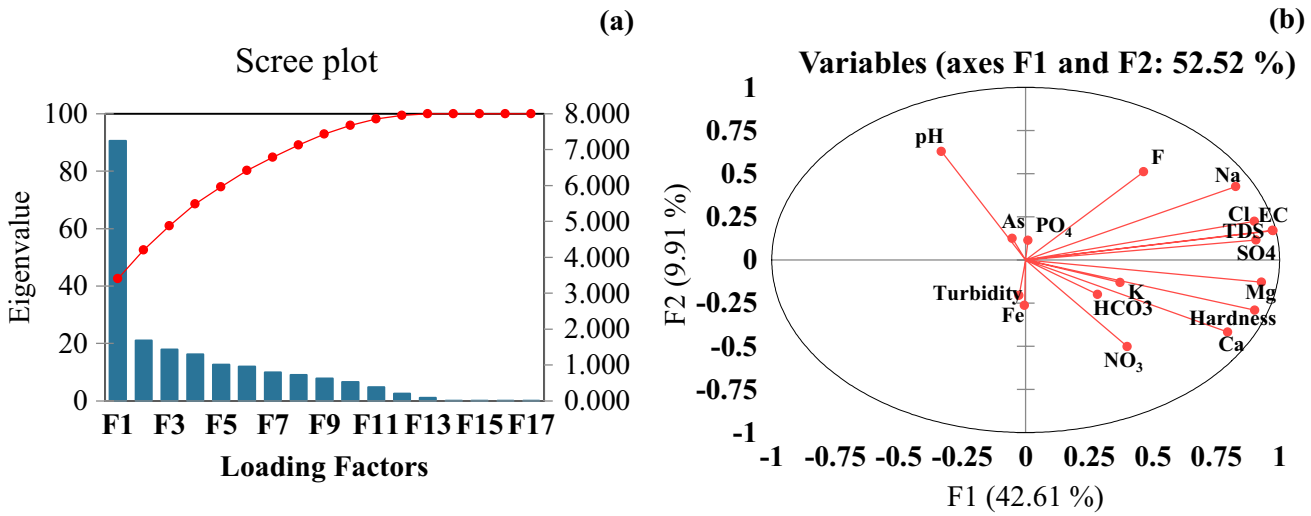

Fig. 4 **a** Sum of all the calculated factors, **b** contribution of the four loading factors F1, F2, F3, and F4 after varimax rotation

with phosphate. Fertilizers and animal or waste product decomposition can add phosphate to groundwater (Liu et al. 2020).

Correlation analysis

The Pearson correlation statistical method is used to understand the geochemical modeling of chemical characteristics (Bhardwaj et al. 2010). The correlation matrix of the physicochemical parameters for groundwater samples is exhibited in Table 3. With a statistical significance level of 0.05, the correlation matrix revealed a good to moderate positive correlation of TDS with major ions Cl^-, SO_4^{2-}, Ca^{2+}, EC, Mg^{2+}, Na^+, and hardness, revealing that these ions influence the chemistry of the groundwater (Appelo and Postma 2005). NO_3^- had a moderate correlation with HCO_3^-, SO_4^{2-}, K^+, Ca^{2+}, and Mg^{2+}, showing anthropogenic input in the groundwater aquifer, possibly due to fertilizer leaching from agricultural lands during farming activities. TDS showed a slight positive correlation with F^- in the current study. Many studies have found that high F^- concentrations are associated with high TDS levels. Evaporation functions as a precursor in F^- release in groundwater because it can restrict Ca^{2+} ions by precipitating $CaCO_3$. As a result, the fluorite mineral's solubility in water is reduced (Younas et al. 2019). With a correlation coefficient of 0.5, Na^+ had a moderate correlation with F^- in this study (Table 3). The presence of F^- due to rock weathering has been confirmed. High Na^+ concentrations can improve the solubility of minerals containing F^-. Furthermore, there was no significant correlation between F^- and Ca^{2+} (Table 3). Fluorite dissolution could be caused by low Ca^{2+} and Mg^{2+} ion concentrations caused by precipitation such as calcite and dolomite. The weak correlation between F^- and Ca^{2+} indicates that F^- contamination is primarily caused by mineral fluorite CaF_2 and the subsequent cation exchange reactions (Na^+ is exchanged for Ca ion), which govern groundwater F^- chemistry (Bhattacharya et al. 2020).

Major factors controlling hydrogeochemical processes

Various variables greatly influence hydrogeochemical processes, such as groundwater regime, aquifer lithology, and climatic conditions. The Gibbs diagram can determine the lithology-hydrochemistry relationship in aquifers (Jat Baloch et al. 2021a). Figure 5a depicts that most of the groundwater samples are found in the rock-dominance and evaporation-dominance regions, indicating that these processes primarily regulate groundwater hydrochemistry. In the study region, the input of soluble ions from atmospheric precipitation is negligible because of the arid climate and rare rainfall. The hydrochemical components of groundwater mainly come from the weathering hydrolysis of minerals (Fig. 5a). High F^- in groundwater is more strongly affected by evaporation compared to low F^- groundwater (Fig. 5a), which could be demonstrated by the local arid climate. The relationship between $\gamma(Ca^{2+}/Na^+)$ and $\gamma(HCO_3^-/Na^+)$ can be used to determine the source of major ions in the groundwater (Li et al. 2015). It is seen from Fig. 5b, the groundwater samples are mainly distributed near the end members of silicate minerals and close to the end members of evaporites, indicating that the hydrochemical compositions of groundwater mainly originated from the dissolution of evaporites and the weathering hydrolysis of silicate minerals, and relatively less affected by the weathering of carbonate rocks. Thus, the abundance of F^- in the groundwater of our study area may have resulted from the release of fluoride-containing minerals, including silicates.

The milligram equivalent ratio of Cl^- to Na^+ in most samples was less than 1 (Fig. 6a), indicating that the milligram equivalent concentration of Na^+ is much higher than that of Cl^-. In addition to the dissolution of halite, the Na^+ in groundwater may also originate from the dissolution of silicate and Na^+-Ca^{2+} exchange (Gugulothu et al. 2022b). Silicate rock weathering is a major contributor to high levels of sodium (Na^+) in groundwater. The alternating adsorption of cations may influence it.

$(Ca^{2+} + Mg^{2+})/(HCO_3^- + SO_4^{2-})$ milligram equivalent ratio can speculate the source of Ca^{2+}, Mg^{2+}, and SO_4^{2-} (Li et al. 2015). As depicted in Fig. 6b, the ratios of most samples below the 1:1 relation line indicate that Ca^{2+}, Mg^{2+}, and SO_4^{2-} are primarily derived from the weathering and filtration control of evaporite and silicate minerals. Most samples were distributed above the 1:1 line (Fig. 6c), confirming groundwater chemical formation. The controlling factor is the dissolution of evaporite minerals, and the sample points distributed below the 1:1 line may be accompanied by carbonate dissolution.

The plot of $(Ca^{2+} + Mg^{2+}\text{-}HCO_3^-\text{-}SO_4^{2-})$ versus $(Na^+\text{-}Cl^-)$ demonstrates the involvement of Na^+, Ca^{2+}, and Mg^{2+} in the ion exchange reaction (Fig. 6d). Ca^{2+} or Mg^{2+} added or removed from the groundwater system due to carbonate or gypsum dissolution is represented by $(Ca^{2+} + Mg^{2+}\text{-}HCO_3^-\text{-}SO_4^{2-})$. In contrast, the amount of Na^+ added or lost due to halite dissolution is represented by Na-Cl (Rao et al. 2022a). According to the slope, Ca^{2+}, Na^+, and Mg^{2+} are involved in the reverse ion exchange process derived from interaction with the aquifer material (Gugulothu et al. 2022b).

Genesis of fluoride and nitrate in groundwater

F^- in the groundwater of the research region originates from fluoride-bearing minerals (fluorite), which will be mobilized

Table 3 Pearson correlation matrix of the study area's physiochemical parameters for groundwater

	pH	EC	TDS	Turbidity	Hardness	F	Cl	NO_3	HCO_3	SO_4	PO_4	Ca	Mg	Na	K	Fe	As
pH	1																
EC	−0.234**	1															
TDS	−0.233**	**0.999****	1														
Turbidity	−0.001	−0.028	−0.03	1													
Hardness	−0.399**	0.806**	0.**806****	0.019	1												
F	0.138	0.469**	0.479**	−0.076	0.248**	1											
Cl	−0.211**	**0.960****	**0.952****	−0.018	**0.728****	0.382**	1										
NO_3	−0.301**	0.295**	0.303**	−0.048	0.415**	0.087	0.203**	1									
HCO_3	−0.200*	0.191*	0.199*	−0.113	0.272**	0.351**	0.038	0.270**	1								
SO_4	−0.199*	**0.885****	0.**897****	0.003	0.**793****	0.474**	**0.759****	0.268**	0.178*	1							
PO_4	−0.132	0.023	0.016	−0.048	0.004	0.002	0.079	−0.079	−0.091	−0.038	1						
Ca	−0.433**	0.**682****	0.**680****	0.014	**0.956****	0.142	**0.619****	0.436**	0.226**	**0.666****	−0.002	1					
Mg	−0.326**	**0.861****	0.**863****	0.021	0.**952****	0.336**	**0.774****	0.354**	0.296**	0.**853****	0.007	**0.821****	1				
Na	−0.097	**0.926****	**0.925****	−0.049	0.532**	0.**522****	**0.916****	0.165*	0.132	**0.771****	0.033	0.380**	0.**642****	1			
K	−0.107	0.325**	0.333**	−0.039	0.286**	0.112	0.266**	0.248**	0.129	0.339**	−0.105	0.231**	0.317**	0.213**	1		
Fe	−0.07	0.431	0.001	0.301**	−0.018	−0.055	0.005	0.082	−0.037	−0.012	−0.162*	0.004	−0.039	0.006	0.034	1	
As	0.023	−0.047	−0.045	−0.15	−0.073	0.09	−0.079	0.059	−0.003	−0.039	0.021	−0.112	−0.022	−0.028	0.025	0.009	1

*Correlation is significant at the 0.01 level (2-tailed). Bold = strong correlation (> 0.90)

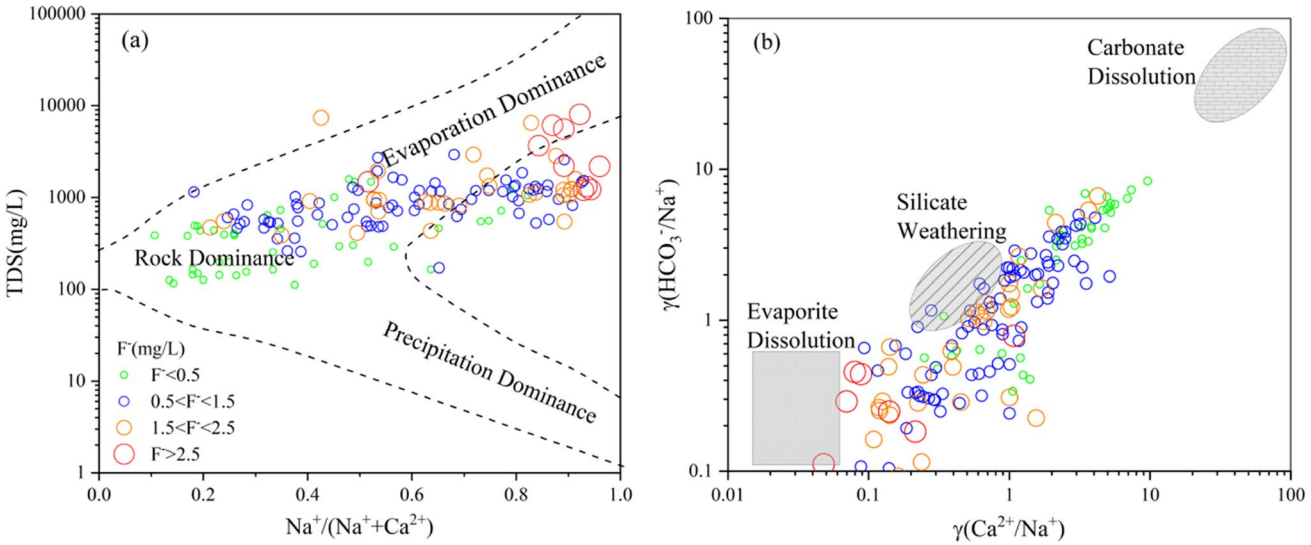

Fig. 5 $Na^+/(Na^+ + Ca^{2+})$ mg/L versus Log TDS (**a**) and Na-normalized HCO_3^- versus Na-normalized $Ca.^{2+}$ (mM/mM) (**b**)

in the groundwater under ideal alkalinity and temperature conditions. The solubility of fluorite is pH dependent; the pH of groundwater varied from 6.7 to 8.55, with a mean of 7.72, indicating favorable weak alkaline conditions for F^- enrichment in the study region (Fig. 7a). As shown in Fig. 7b, F^- concentration increases with the increase of HCO_3^- concentration in groundwater. Due to increased OH^- content, CaF_2 dissolves in alkaline or slightly alkaline groundwater (Chen et al. 2017). HCO_3^- in groundwater can promote fluorinated mineral dissolution (Eq. 5) and increase the level of F^- in groundwater.

$$CaF_2 + 2HCO_3^- = CaCO_3 + 2F^- + H_2O + CO_2 \quad (5)$$

Schoeller (1965) demonstrated the possibility of cation exchange using two indexes, CAI-1 and CAI-2 (Xu et al. 2022), and their calculation methods were shown in Eqs. 6 and 7, respectively. CAI-1 and CAI-2 will be positive when Na^+ and K^+ in water exchange Ca^{2+} and Mg^{2+}. When Ca^{2+} and Mg^{2+} exchange adsorbed Na^+ and K^+ in the water, the values of CAI-1 and CAI-2 are negative, and the effect of cation exchange is more pronounced when the absolute value of CAI-1 and CAI-2 is larger. Figure 7c shows that approximately half of the two indexes, F^- are negative, confirming the presence of cation exchange of Na^+ and K^+ in the adsorbed state of Ca^{2+} and Mg^{2+} in the elevated F^- groundwater in the study area. The decreased Ca^{2+} concentration in groundwater caused by cation exchange promotes fluoride enrichment in groundwater.

$$\text{CAI-1} = \frac{Cl^- - \left(Na^+ + K^+\right)}{Cl^-} \quad (6)$$

$$\text{CAI-2} = \frac{Cl^- - \left(Na^+ + K^+\right)}{HCO_3^- + SO_4^{2-} + CO_3^{2-} + NO_3^-} \quad (7)$$

Furthermore, as shown in Fig. 7d, the correlation between F^- and Ca^{2+}, groundwater with a high Ca^{2+} content preferred low F^- concentrations (Narsimha and Sudarshan 2017). These results indicated that Ca^{2+} could inhibit F^-. Because Ca^{2+} has a strong affinity with HCO_3^-, $CaCO_3$ precipitates, which reduces Ca^{2+} in groundwater and speeds up the fluorite dissolution (Eq. 5), thus increasing the level of F^- in the groundwater.

Positive relationships between F^- and pH and HCO_3^- and a negative relationship between F^- and Ca^{2+} often accelerate F^- content in groundwater, indicating fluorite-saturated groundwater concentrations (Ayoob and Gupta 2006; Rao et al. 2021; Xiao et al. 2022a). As shown in Fig. 8a, the groundwater was supersaturated for calcite and dolomite and unsaturated for fluorite and gypsum in the study area. Calcite and dolomite precipitation reduces Ca^{2+} in groundwater, which promotes fluorite dissolution and increases F^- concentration in groundwater. The unsaturation of gypsum encourages the precipitation of calcite and, thus, the dissolution of fluorite. Fluorite weathering is the critical source of F^- in the aquifers, as evidenced by their significant positive correlation.

The fluorite dissolution equilibrium shifts toward precipitation when the activity of Ca^{2+} and F^- in solution exceeds the fluorite dissolution equilibrium constant (Yan et al. 2020). Groundwater samples are concentrated below the fluorite dissolution equilibrium line (pKfluorite = 10.6) (Fig. 8b), implying that fluorite content in the groundwater is controlled by fluorite solubility in the study region. When

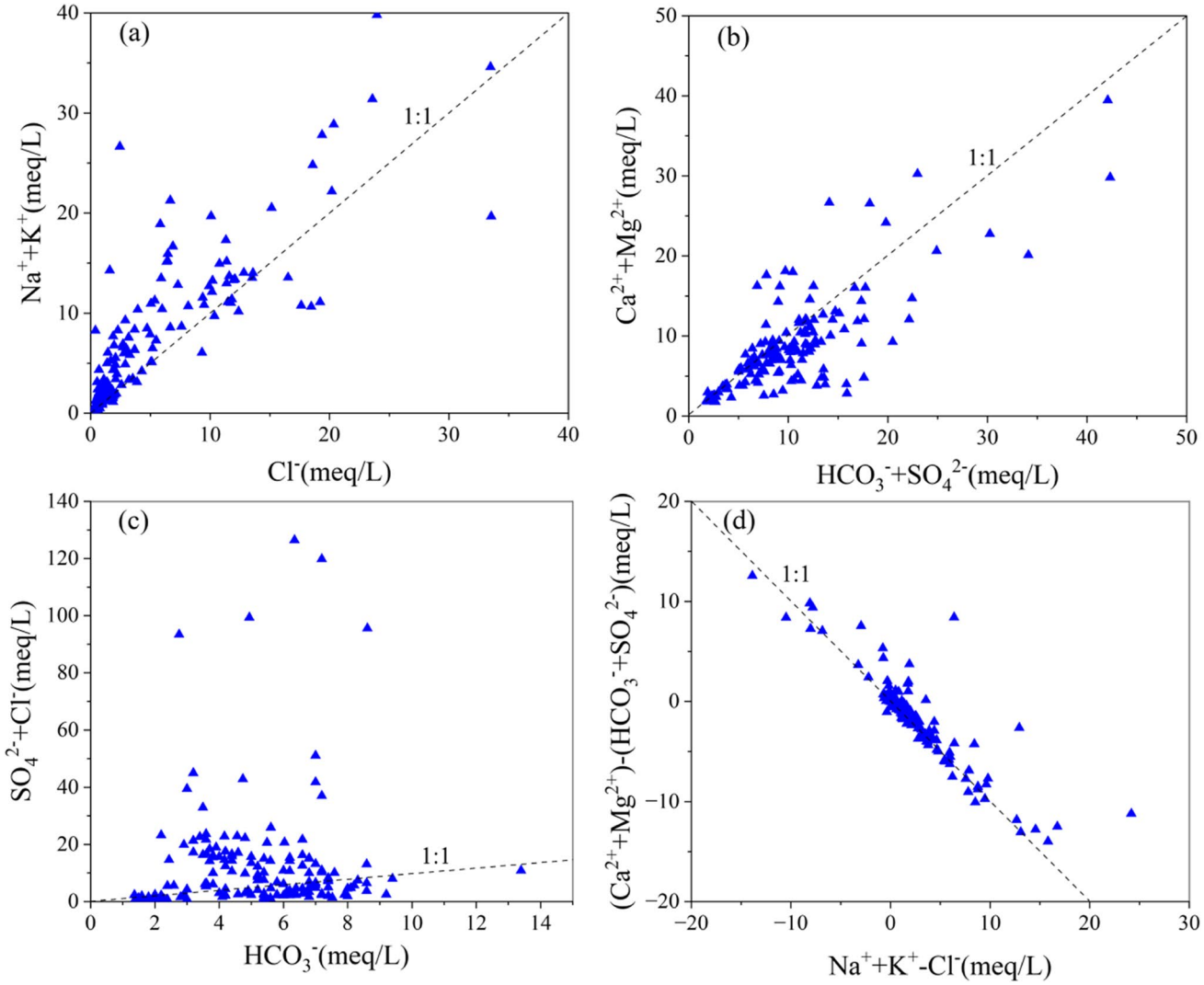

Fig. 6 Ionic ratio plots

only fluorite was dissolved, F^- and Ca^{2+} activity increased along trend line 1; most samples were found to the right of trend line 1, revealing that the Ca^{2+} in the groundwater came from sources other than fluorite. When only fluorite was dissolved, F^- and Ca^{2+} activity increased along trend line 1; most samples were found to the right of trend line 1, revealing that Ca^{2+} in the groundwater came from sources other than fluorite (Li et al. 2018). Given that groundwater contains large amounts of HCO_3^- and SO_4^{2-}, this Ca^{2+} may come from dissolved calcite, dolomite, and gypsum. When calcite and fluorite were dissolved in a 200:1 mass ratio, the activity of F^- and Ca^{2+} increased along trend line 2, and the majority of water samples were located between trend lines 1 and 2, indicating that the concentration of F^- was controlled by Ca^{2+} from dissolved sources of fluorite, calcite, gypsum, and other minerals (Luo et al. 2018).

The pattern of groundwater flow is based on quaternary topography. As a result, groundwater chemistry differs in each of the three groundwater flow paths (I, II, and III), including EC, pH, TDS, turbidity, TH, Na^+, PO_4^{3-}, K^+, Mg^{2+}, Cl^-, HCO_3^-, SO_4^{2-}, F^-, and Ca^{2+} are presented in Table S1. It indicates that the F^- content in groundwater generally decreases along the groundwater flow path, reaching up to 2.64 mg/L from path I to path II. The decreasing trend investigated is due to an increase in Ca^{2+} from the path I to the central path (II), whereas groundwater Mg^{2+} shows a decreasing trend from path I to the central path (II). It may be related to the continental salinization that occurred in the central zones of the flow-path II, and the dissolution of evaporate minerals causes an increase in salinity in groundwater (Li et al. 2020). Geochemical inverse modeling was utilized to better understand the effects of hydrogeochemical evolution along groundwater flow paths

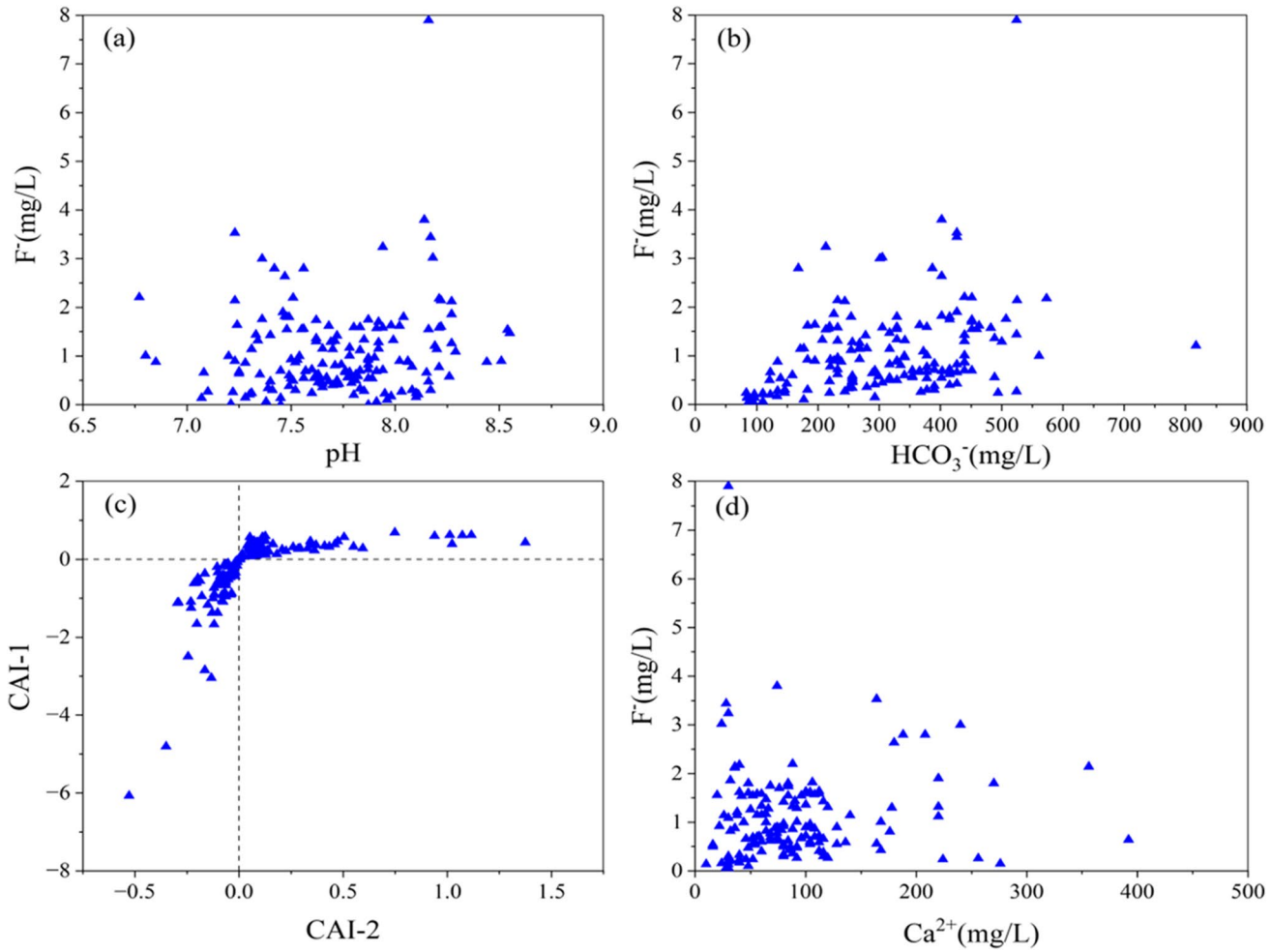

Fig. 7 Cross plots of fluoride versus other parameters and CAI-1 vs. CAI-2

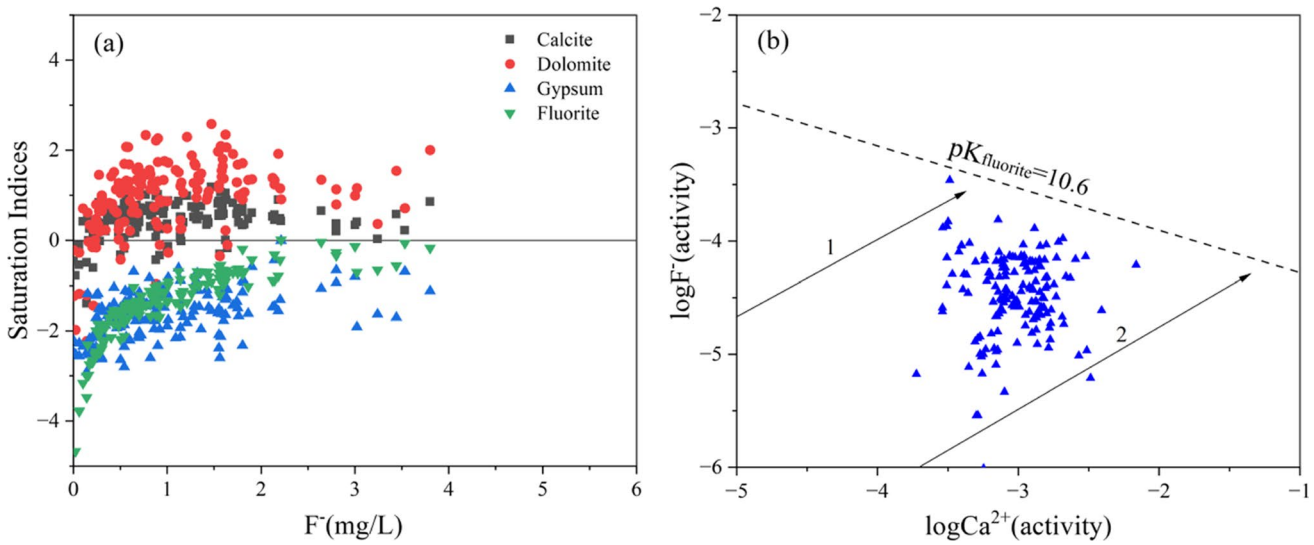

Fig. 8 SI of calcite, dolomite, gypsum, and fluorite in groundwater (**a**) $logF^{-}$ (activity) vs. $LogCa.^{2+}$ (activity) (**b**)

on F^- mobilization, and the solid phase was established based on the sediment mineralogy of the research location (Haji et al. 2018). It is primarily comprised of four hydrogeochemical processes: (1) fluorite dissolution, which is the primary source of fluoride in the groundwater of the study area, (2) calcite and dolomite dissolution precipitation, (3) cation exchange between Na^+ and Ca/Mg on the clay, and (4) chemical weathering.

NO_3^- concentrations ranged from 0.1 to 70 mg/L, with an average of 8.89 mg/L. The permissible limit of 50 mg/L (WHO 2022) was exceeded in approximately 3.74% of the groundwater samples (Fig. 3). Agrochemicals damage soil and cause increased nitrate leaching, causing NO_3^- to accumulate in the groundwater. Fertilizer use is common in the area, resulting in high NO_3^- levels in the groundwater (Nemčić-Jurec and Jazbec 2017). Nitrogen-rich sediments, organic nitrogen inputs into soil, groundwater contamination with nitrogen-rich wastes, biological denitrogenating fixation by microorganisms, animal and human waste, water in unutilized dug wells, nitrogenous inorganic fertilizers, and stagnant water are the common sources of NO_3^- in groundwater (Rezaei et al. 2017). Agriculture is also one of the primary activities in the research region, and it is predicted that many applied agrochemicals will permeate the soil and reach groundwater. As a result, the amount of NO_3^- in groundwater is likely to rise (Rao et al. 2022a). The high NO_3^- level in the groundwater is caused by agricultural activities in the study area's southern, northern, eastern, and central regions, according to a spatial distribution map of NO_3^- (Fig. 3).

The similar spatial distribution of K^+, Cl^-, and NO_3^- was used to identify anthropogenic activities (Rezaei et al. 2017; Wang et al. 2021; Yadav et al. 2018). In Fig. 9a, most of the samples were distributed near the end members of domestic sewage and tended to be close to the end members of agricultural pollution. Results indicated that domestic sewage and agricultural fertilizer pollution significantly impacted nitrate contamination of groundwater in the study region. A few samples are close to evaporite endmembers, indicating that NO_3^- enrichment in groundwater is also influenced by geological factors to a certain extent.

Since there is a strong correlation between NO_3^- from fertilizer and K^+, to find the important cause of the elevated nitrate in the groundwater (Kom et al. 2022; Xiao et al. 2022b), the relationship diagram of NO_3^- and K^+ (Fig. 9b) shows that there is no significant correlation between NO_3^- and K^+ in most groundwater samples. When NO_3^- concentration is low, the content of K^+ is low and high; only a small number of groundwater samples have a positive correlation between NO_3^- and K^+. The discharge of domestic sewage is the critical source of NO_3^- pollution in the groundwater of the study area and is also affected by agricultural fertilizers. In addition, it can be seen that most of the high nitrate groundwaters (nitrate content > 50 mg/L) were plotted in the mixed Cl-Mg-Ca, Cl-Na, and mixed HCO_3-Na-Ca dominance (Fig. 2b). Therefore, it can be concluded that high NO_3^- contamination typically comes from external sources. These external sources also introduce major ions into aquifers, leading to the evolution of groundwater with a salty hydrochemical composition.

Non-carcinogenic health risk assessment

The EDI, HQ, and THI values for adults and children were calculated through drinking water ingestion and are summarized in Table 4. The mean EDI values of F^- and NO_3^- were < 1 for the adults and children, respectively. The

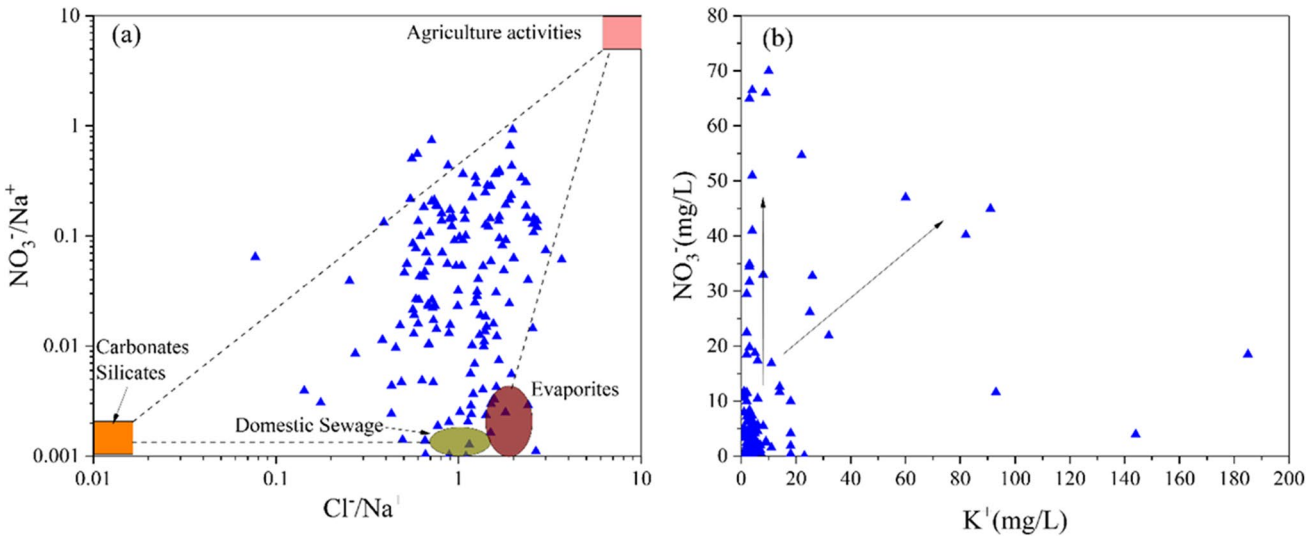

Fig. 9 Plots of $Cl^-/Na+$ vs. NO_3^-/Na^+ (**a**) and NO_3^- vs. $K.^+$ for groundwater samples (**b**)

Table 4 Results of the non-carcinogenic risks of fluoride and nitrate via ingestion of drinking water

	F				NO_3			
	EDI		HQing		EDI		HQing	
	Adults	Children	Adults	Children	Adults	Children	Adults	Children
Min	5.71E−04	1.19E−03	9.52E−03	1.98E−02	3.57E−03	6.67E−03	2.23E−03	4.17E−03
Max	2.26E−01	4.69E−01	3.76E+00	7.81E+00	2.50E+00	4.67E+00	1.56E+00	2.92E+00
Average	3.09E−02	6.41E−02	5.14E−01	1.07E+00	3.17E−01	5.93E−01	1.98E−01	3.70E−01
THI	–	–	8.18E+01	1.70E+02	–	–	3.19E+01	5.96E+01

HQ values of F^- ranged from 9.52E−03 to 3.76E+00, 1.98E−02 to 7.81E+00, and the average values of 5.14E−01 and 1.07E+00 for the adults and children, respectively. In contrast, the HQ values of NO_3^- varied from 2.23E−03 to 1.56E+00 and 4.17E−03 to 2.92E+00 with average values of 1.98E−01 and 3.70E−01, respectively. High HQ values of F^- were observed (> 1) for the adults and children of the local population in the sub-regions, including Nari Zone-B, Pindi Waheer, Chak no 5, Rukhla, Katha Sagral, Mangowal, Diawal, Jassowal, Kund DeraJat, Waracha, Fateh Pur Maira, Golay Wali Dera Jat, Muhammdkhel, Chak, Jalalpur, Katha Misseral, Ochala, Dhadhar Dera, Ghatti, and Badli Wala. In contrast, the NO_3^- had high HQ values (> 1) for adults and children in sub-regions. Pindi Waheer, Kund Dera Jat, Mitha Twana, Chak, Nomi Wali, Khair Pur, Ochala, Kuffari, Jahlar, and Khottaka indicate a high risk of F^- and NO_3^- contamination. In contrast, it was observed that the risk involved in the remaining regions is low and negligible for the local population.

The THI mean values of F^- were 8.18E+01 and 1.70E+02, while the mean values of NO_3^- for the adults and children were 3.19E+01 and 5.96E+01, respectively. The results showed that 40% of the samples exceeded the THI > 1 for adults and children as shown in Table 4, indicating high non-carcinogenic risk (THI > 1) for the local population in the study area. Based on the non-carcinogenic risk of HQ and THI results, adults and children are at greater risk. Consequently, F^- exhibits a high non-carcinogenic risk (> 1) as compared to NO_3^- based on the elevated concentration, which is prone to cause health problems, such as skeletal fluorosis and dental issues in infants (Magne et al. 2020). Moreover, high F^- concentration causes fluorosis, spinal disorders, and teeth and bone diseases by continuously ingesting contaminated groundwater (Yousefi et al. 2018). The high non-carcinogenic risk of NO_3^- (> 1) via drinking water consumption resulted in colorectal cancer, childhood central nervous system tumors, thyroid disorders, and neural tube defects (Ransom et al. 2022). The dental and skeletal fluorosis cases were observed in the study area as shown in Fig. 10. Consequently, elevated concentrations of F^- and NO_3^- pose a health risk to the population in the study region, as the total number of water samples in sub-regions represents the entire Khushab district.

Fig. 10 Symptoms of dental and skeletal due to fluoride exposure in the study area

Conclusion

Elevated F^- and NO_3^- concentrations in groundwater and the associated non-carcinogenic health risk for children and adults were investigated in the Khushab region using hydrogeochemical, (geo)statistical, and multivariate approaches. The groundwater is neutral to alkaline. Most of the major ions were found within the allowable drinking water limits in most groundwater samples, but F^- and NO_3^- contaminants were found beyond the acceptable drinking water limits in 25.46% and 3.73% of the sampled groundwater, respectively. The hydrochemical compositions of groundwater are primarily the result of silicate weathering, carbonate dissolution, cation exchange, dissolution of evaporites, and anthropogenic activities. Evaporation plays a crucial role in the formation of high F^- shallow groundwater. Mixing with shallow groundwater provides additional F^- into deep groundwater. The dissolution of fluorine-containing minerals and naturally HCO_3-Na type groundwater resulted in high F^- groundwater. The NO_3^- concentration is highest in mixed Cl-Mg-Ca and mixed HCO_3-Na-Ca type water. The NO_3^- contaminant usually originates from external inputs. Domestic sewage discharge is the primary source of NO_3^- pollution in the study area, exacerbated by agricultural fertilizer pollution. As a result, external sources of NO_3^- contamination introduce major ions into aquifers, causing the evolution of groundwater toward a salty hydrochemical composition. F^- and NO_3^- exhibited high non-carcinogenic risk ($HQ > 1$) and ($THI > 1$) for adults and children, indicating an increased health risk to the local population. The study suggests taking practical measures to enhance safe drinking water management, such as denitrification, defluoridation, implementing methods for harvesting rainwater, providing sanitary facilities, and limiting the use of chemical fertilizers, to protect groundwater resources from pollution and enhance the health of the residents. To reduce health risks, proper preventive measures must be implemented, including enhancing sanitation facilities and limiting the use of agricultural chemicals to prevent NO_3^- pollution of the aquifer system, and filters to remove F^- to improve human health. The findings of this study will assist decision-makers in the Khushab district of Pakistan in developing long-term plans for groundwater resource development.

Supplementary Information The online version contains supplementary material available at https://doi.org/10.1007/s11356-023-25958-x.

Acknowledgements The authors gratefully acknowledge the help of anonymous peer reviewers and the editors for their valuable comments.

Author contribution All authors contributed to the study's conception and design. The first draft of the manuscript was written by Javed Iqbal, supervision, material preparation, and manuscript revision (Chunli Su, Mengzhu Wang, Hasnain Abbas, Muhammad Yousuf Jat Baloch, Junaid Ghani, Zahid Ullah, Md. Enamul Huq) and all authors commented on previous versions of the manuscript. All authors read and approved the final manuscript.

Funding The research work was supported by the National Key R&D Program of China (2022YFC2503001) and the National Natural Science Foundation of China (Grant 42177078 and 41521001).

Data availability The data will be provided on request to the corresponding author.

Declarations

Ethics approval Not applicable.

Consent to participate All authors reviewed and approved the final manuscript.

Consent for publication All authors approved this for publication.

Competing interests The authors declare no competing interests.

References

Abbas Z, Mapoma HWT, Su C, Aziz SZ, Ma Y, Abbas N (2018) Spatial analysis of groundwater suitability for drinking and irrigation in Lahore, Pakistan. Environ Monit Assess 190:1–16

Adams S, Titus R, Pietersen K, Tredoux G, Harris C (2001) Hydrochemical characteristics of aquifers near Sutherland in the Western Karoo, South Africa. J Hydrol 241:91–103

Adimalla N, Li P, Qian H (2018) Evaluation of groundwater contamination for fluoride and nitrate in semi-arid region of Nirmal Province, South India: a special emphasis on human health risk assessment (HHRA). Hum Ecol Risk Assess Int J. https://doi.org/10.1080/10807039.2018.1460579

Ahada CP, Suthar S (2019) Assessment of human health risk associated with high groundwater fluoride intake in southern districts of Punjab, India. Exposure and Health 11:267–275

Ahmad M, Jamal A, Tang X-W, Al-Sughaiyer MA, Al-Ahmadi HM, Ahmad F (2020) Assessing potable water quality and identifying areas of waterborne diarrheal and fluorosis health risks using spatial interpolation in Peshawar. Pak Water 12:2163

Akram M (2014) Citric acid cycle and role of its intermediates in metabolism. Cell Biochem Biophys 68:475–478

Alam K, Ahmad N (2014) Determination of aquifer geometry through geophysical methods: a case study from Quetta Valley, Pakistan. Acta Geophys 62:142–163

Al-Rasheed M (2013) A most masculine state: gender, politics and religion in Saudi Arabia. Cambridge University Press, Cambridge

Anjum MN, Shah MT, Ali F, Hussain E, Ali L (2013) Geochemical studies of fluoride in drinking water of Union Council Ganderi, district Nowshera, Khyber Pakhtunkhwa, Pakistan. World Appl Sci J 27:632–636

Appelo C, Postma D (2005): Groundwater and pollution. Rotterdam

Aurrecoechea C, Brestelli J, Brunk BP, Dommer J, Fischer S, Gajria B, Gao X, Gingle A, Grant G, Harb OS (2009) PlasmoDB: a

functional genomic database for malaria parasites. Nucleic Acids Res 37:D539–D543
Ayoob S, Gupta AK (2006) Fluoride in drinking water: a review on the status and stress effects. Crit Rev Environ Sci Technol 36:433–487
Azis A (2015) Conceptions and practices of assessment: a case of teachers representing improvement conception. Teflin J 26:129–154
Baloch MYJ, Mangi SH (2019) Treatment of synthetic greywater by using banana, orange and sapodilla peels as a low cost activated carbon. J Mater Environ Sci 10:966–986
Baloch MYJ, Talpur SA, Talpur HA, Iqbal J, Mangi SH, Memon S (2020) Effects of arsenic toxicity on the environment and its remediation techniques: a review. J Water Environ Technol 18:275–289
Baloch MYJ, Su C, Talpur SA, Iqbal J, Bajwa K (2022) Arsenic removal from groundwater using iron pyrite: influences factors and removal mechanism J Earth Sci
Beaver JR, Manis EE, Loftin KA, Graham JL, Pollard AI, Mitchell RM (2014) Land use patterns, ecoregion, and microcystin relationships in US lakes and reservoirs: a preliminary evaluation. Harmful Algae 36:57–62
Bhardwaj V, Singh DS, Singh A (2010) Hydrogeochemistry of groundwater and anthropogenic control over dolomitization reactions in alluvial sediments of the Deoria district: Ganga plain, India. Environ Earth Sci 59:1099–1109
Bhattacharya P, Adhikari S, Samal AC, Das R, Dey D, Deb A, Ahmed S, Hussein J, De A, Das A (2020) Health risk assessment of co-occurrence of toxic fluoride and arsenic in groundwater of Dharmanagar region, North Tripura (India). Groundw Sustain Dev 11:100430
Brindha K, Elango L (2011) Fluoride in groundwater: causes, implications and mitigation measures. Fluoride Prop Applic Environ Manag 1:111–136
Chaudhari N, Talwar P, Parimisetty A, Lefebvre d'Hellencourt C, Ravanan P (2014) A molecular web: endoplasmic reticulum stress, inflammation, and oxidative stress. Front Cell Neurosci 8:213
Cheema M, Bastiaanssen WG (2010) Land use and land cover classification in the irrigated Indus Basin using growth phenology information from satellite data to support water management analysis. Agric Water Manag 97:1541–1552
Chen J, Wu H, Qian H, Gao Y (2017) Assessing nitrate and fluoride contaminants in drinking water and their health risk of rural residents living in a semiarid region of northwest China. Expo Health 9:183–195
Chen Q, Jia C, Wei J, Dong F, Yang W, Hao D, Jia Z, Ji Y (2020) Geochemical process of groundwater fluoride evolution along global coastal plains: evidence from the comparison in seawater intrusion area and soil salinization area. Chem Geol 552:119779
Dilpazeer F, Munir M, Baloch MYJ, Shafiq I, Iqbal J, Saeed M, Abbas MM, Shafique S, Aziz KHH, Mustafa A, Mahboob I (2023) A comprehensive review of the latest advancements in controlling arsenic contaminants in groundwater. 15:478
Farooqi A, Masuda H, Firdous N (2007) Toxic fluoride and arsenic contaminated groundwater in the Lahore and Kasur districts, Punjab, Pakistan and possible contaminant sources. Environ Pollut 145:839–849
Gelfand MJ, Raver JL, Nishii L, Leslie LM, Lun J, Lim BC, Duan L, Almaliach A, Ang S, Arnadottir J (2011) Differences between tight and loose cultures: a 33-nation study. Science 332:1100–1104
Ghani J, Ullah Z, Nawab J, Iqbal J, Waqas M, Ali A, Almutairi M, Peluso I, Mohamed H, Shah M (2022) Hydrogeochemical characterization, and suitability assessment of drinking groundwater: application of geostatistical approach and geographic information system. Front Environ Sci 10:874464
Greenman DW, Bennett GD, Swarzenski WV (1967) Ground-water hydrology of the Punjab, West Pakistan, with emphasis on problems caused by canal irrigation, 1. US Government Printing Office
Gugulothu S, Subba Rao N, Das R, Duvva LK, Dhakate R (2022a) Judging the sources of inferior groundwater quality and health risk problems through intake of groundwater nitrate and fluoride from a rural part of Telangana, India. Environ Sci Pollut Res 29:49070–49091. https://doi.org/10.1007/s11356-022-18967-9
Gugulothu S, Subbarao N, Das R, Dhakate R (2022b) Geochemical evaluation of groundwater and suitability of groundwater quality for irrigation purpose in an agricultural region of South India. Appl Water Sci 12:1–13
Haji M, Wang D, Li L, Qin D, Guo Y (2018) Geochemical evolution of fluoride and implication for F− enrichment in groundwater: example from the Bilate River Basin of Southern Main Ethiopian Rift. Water 10:1799
Haji M, Karuppannan S, Qin D, Shube H, Kawo NS (2021) Potential human health risks due to groundwater fluoride contamination: a case study using multi-techniques approaches (GWQI, FPI, GIS, HHRA) in Bilate River Basin of Southern Main Ethiopian Rift, Ethiopia. Arch Environ Contam Toxicol 80:277–293
Herczeg A, Dogramaci S, Leaney F (2001) Origin of dissolved salts in a large, semi-arid groundwater system: Murray Basin, Australia. Mar Freshw Res 52:41–52
Huq ME, Fahad S, Shao Z, Sarven MS, Khan IA, Alam M, Saeed M, Ullah H, Adnan M, Saud S (2020) Arsenic in a groundwater environment in Bangladesh: occurrence and mobilization. J Environ Manage 262:110318
Hussain Y, Ullah SF, Hussain MB, Aslam AQ, Akhter G, Martinez-Carvajal H, Cárdenas-Soto M (2017) Modelling the vulnerability of groundwater to contamination in an unconfined alluvial aquifer in Pakistan. Environ Earth Sci 76:1–11
Inyang M, Gao B, Yao Y, Xue Y, Zimmerman AR, Pullammanappallil P, Cao X (2012) Removal of heavy metals from aqueous solution by biochars derived from anaerobically digested biomass. Biores Technol 110:50–56
Iqbal J, Su C, Rashid A, Yang N, Baloch MYJ, Talpur SA, Ullah Z, Rahman G, Rahman NU, Sajjad MM (2021) Hydrogeochemical assessment of groundwater and suitability analysis for domestic and agricultural utility in Southern Punjab, Pakistan. Water 13:3589
Jat Baloch MY, Zhang W, Chai J, Li S, Alqurashi M, Rehman G, Tariq A, Talpur SA, Iqbal J, Munir M (2021a) Shallow groundwater quality assessment and its suitability analysis for drinking and irrigation purposes. Water 13:3361
Jat Baloch MY, Zhang W, Chai J, Li S, Alqurashi M, Rehman G, Tariq A, Talpur SA, Iqbal J, Munir M (2021) Shallow groundwater quality assessment and its suitability analysis for drinking and irrigation purposes. Water 13:3361
Jat Baloch MY, Zhang W, Shoumik BAA, Nigar A, Elhassan AA, Elshekh AE, Bashir MO, Mohamed Salih Ebrahim AF, Ka Adam Mohamed, Iqbal J (2022a) Hydrogeochemical mechanism associated with land use land cover indices using geospatial, remote sensing techniques, and health risks model. Sustainability 14:16768
Jat Baloch MY, Zhang W, Zhang D, Al Shoumik BA, Iqbal J, Li S, Chai J, Farooq MA, Parkash A (2022b) Evolution mechanism of arsenic enrichment in groundwater and associated health risks in southern Punjab, Pakistan. Int J Environ Res Public Health 19:13325
Kamruzzaman M, Alanazi S, Alruwaili M, Alshammari N, Siddiqi M, Huq M (2020) Water resource evaluation and identifying

groundwater potential zones in arid area using remote sensing and geographic information system. J Comput Sci 16:266–279
Khan SS, Xue JL, Kazmi WH, Gilbertson DT, Obrador GT, Pereira BJ, Collins AJ (2005) Does predialysis nephrology care influence patient survival after initiation of dialysis? Kidney Int 67:1038–1046
Khan N, Bano A, Zandi P (2018) Effects of exogenously applied plant growth regulators in combination with PGPR on the physiology and root growth of chickpea (Cicer arietinum) and their role in drought tolerance. JPlant Interact 13:239–247
Khattak JA, Farooqi A, Hussain I, Kumar A, Singh CK, Mailloux BJ, Bostick B, Ellis T, van Geen A (2022) Groundwater fluoride across the Punjab plains of Pakistan and India: distribution and underlying mechanisms. Sci Total Environ 806:151353
Kom K, Gurugnanam B, Sunitha V (2022) Delineation of groundwater potential zones using GIS and AHP techniques in Coimbatore district, South India. International Journal of Energy and Water Resources 1–25
Kundu MC, Mandal B (2009) Assessment of potential hazards of fluoride contamination in drinking groundwater of an intensively cultivated district in West Bengal, India. Environ Monit Assess 152:97–103
Lanjwani MF, Khuhawar MY, Khuhawar TMJ, Memon SQ, Samtio MS, Lanjwani AH, Rind IK (2022) Spatial distribution of hydrochemistry and characterization of groundwater of taluka Bakrani, Larkana, Sindh, Pakistan. Arab J Geosci 15:1–24
Li P, Wu J (2019) Drinking water quality and public health. Expo Health 11:73–79
Li C, Gao X, Wang Y (2015) Hydrogeochemistry of high-fluoride groundwater at Yuncheng Basin, northern China. Sci Total Environ 508:155–165
Li D, Gao X, Wang Y, Luo W (2018) Diverse mechanisms drive fluoride enrichment in groundwater in two neighboring sites in northern China. Environ Pollut 237:430–441
Li C, Gao X, Liu Y, Wang Y (2019) Impact of anthropogenic activities on the enrichment of fluoride and salinity in groundwater in the Yuncheng Basin constrained by Cl/Br ratio, δ18O, δ2H, δ13C and δ7Li isotopes. J Hydrol 579:124211
Li J, Wang Y, Zhu C, Xue X, Qian K, Xie X, Wang Y (2020) Hydrogeochemical processes controlling the mobilization and enrichment of fluoride in groundwater of the North China Plain. Sci Total Environ 730:138877
Liu W, Zhang Q, Chen J, Xiang R, Song H, Shu S, Chen L, Liang L, Zhou J, You L (2020) Detection of COVID-19 in children in early January 2020 in Wuhan, China. N Engl J Med 382:1370–1371
Liu X, Wang X, Zhang L, Fan W, Yang C, Li E, Wang Z (2021) Impact of land use on shallow groundwater quality characteristics associated with human health risks in a typical agricultural area in Central China. Environ Sci Pollut Res 28:1712–1724
Luo W, Gao X, Zhang X (2018) Geochemical processes controlling the groundwater chemistry and fluoride contamination in the Yuncheng Basin, China—an area with complex hydrogeochemical conditions. PLoS ONE 13:e0199082
Magne F, Gotteland M, Gauthier L, Zazueta A, Pesoa S, Navarrete P, Balamurugan R (2020) The Firmicutes/Bacteroidetes ratio: a relevant marker of gut dysbiosis in obese patients? Nutrients 12:1474
Masood N, Hudson-Edwards KA, Farooqi A (2022) Groundwater nitrate and fluoride profiles, sources and health risk assessment in the coal mining areas of Salt Range, Punjab Pakistan. Environ Geochem Health 44:715–728
McDonald RI, Douglas I, Revenga C, Hale R, Grimm N, Grönwall J, Fekete B (2011) Global urban growth and the geography of water availability, quality, and delivery. Ambio 40:437–446
Mridha D, Priyadarshni P, Bhaskar K, Gaurav A, De A, Das A, Joardar M, Chowdhury NR, Roychowdhury T (2021) Fluoride exposure and its potential health risk assessment in drinking water and staple food in the population from fluoride endemic regions of Bihar, India. Groundw Sustain Dev 13:100558
Mwiathi NF, Gao X, Li C, Rashid A (2022) The occurrence of geogenic fluoride in shallow aquifers of Kenya Rift Valley and its implications in groundwater management. Ecotoxicol Environ Saf 229:113046
Nabizadehb R, Hadeib M, Zareif A, Asgharib FB, Mohammadic AA (2019) Northwest of Iran as an endemic area in terms of fluoride contamination: a case study on the correlation of fluoride concentration with physicochemical characteristics of groundwater sources in Showt. Desalin Water Treat 155:183–189
Nagendra Rao C (2003) Fluoride and environment—a review. Proceedings of the third international conference on environment and health, Chennai, India. Citeseer, pp 15–17
Narsimha A, Rajitha S (2018) Spatial distribution and seasonal variation in fluoride enrichment in groundwater and its associated human health risk assessment in Telangana State, South India. Hum Ecol Risk Assess Int J 24:2119–2132
Narsimha A, Sudarshan V (2017) Contamination of fluoride in groundwater and its effect on human health: a case study in hard rock aquifers of Siddipet, Telangana State, India. Appl Water Sci 7:2501–2512
Nemčić-Jurec J, Jazbec A (2017) Point source pollution and variability of nitrate concentrations in water from shallow aquifers. Appl Water Sci 7:1337–1348
Puri K, Suresh K, Gogtay N, Thatte U (2009) Declaration of Helsinki, 2008: implications for stakeholders in research. J Postgrad Med 55:131
Purushotham D, Prakash M, Rao AN (2011) Groundwater depletion and quality deterioration due to environmental impacts in Maheshwaram watershed of RR district, AP (India). Environ Earth Sci 62:1707–1721
Qasemi M, Afsharnia M, Farhang M, Ghaderpoori M, Karimi A, Abbasi H, Zarei A (2019) Spatial distribution of fluoride and nitrate in groundwater and its associated human health risk assessment in residents living in Western Khorasan Razavi, Iran. Desalin Water Treat 170:176–186
Qasemi M, Farhang M, Morovati M, Mahmoudi M, Ebrahimi S, Abedi A, Bagheri J, Zarei A, Bazeli J, Afsharnia M (2022) Investigation of potential human health risks from fluoride and nitrate via water consumption in Sabzevar, Iran. Int J Environ Anal Chem 102:307–318
Qasemi M, Darvishian M, Nadimi H, Gholamzadeh M, Afsharnia M, Farhang M, Allahdadi M, Darvishian M, Zarei A (2023) Characteristics, water quality index and human health risk from nitrate and fluoride in Kakhk city and its rural areas. Iran J Food Compos Anal 115:104870
Rafique T, Naseem S, Usmani TH, Bashir E, Khan FA, Bhanger MI (2009) Geochemical factors controlling the occurrence of high fluoride groundwater in the Nagar Parkar area, Sindh, Pakistan. J Hazard Mater 171:424–430
Rafique T, Naseem S, Ozsvath D, Hussain R, Bhanger MI, Usmani TH (2015) Geochemical controls of high fluoride groundwater in Umarkot sub-district, Thar Desert, Pakistan. Sci Total Environ 530:271–278
Rahman NU, Song H, Benzhong X, Rehman SU, Rehman G, Majid A, Iqbal J, Hussain G (2022) Middle-Late Permian and early Triassic foraminiferal assemblages in the Western Salt Range, Pakistan. Rudarsko-geološko-naftni zbornik 37
Raju NJ (2006) Iron contamination in groundwater: a case from Tirumala-Tirupati environs, India. Researcher 1:28–31
Ransom KM, Nolan BT, Stackelberg P, Belitz K, Fram MS (2022) Machine learning predictions of nitrate in groundwater used for

drinking supply in the conterminous United States. Sci Total Environ 807:151065
Rao NS, Dinakar A, Kumari BK (2021) Appraisal of vulnerable zones of non-cancer-causing health risks associated with exposure of nitrate and fluoride in groundwater from a rural part of India. Environ Res 202:111674
Rao NS, Das R, Gugulothu S (2022a) Understanding the factors contributing to groundwater salinity in the coastal region of Andhra Pradesh, India. J Contam Hydrol 250:104053
Rao NS, Dinakar A, Sun L (2022b) Estimation of groundwater pollution levels and specific ionic sources in the groundwater, using a comprehensive approach of geochemical ratios, pollution index of groundwater, unmix model and land use/land cover–a case study. J Contam Hydrol 248:103990
Rao NS, Sunitha B, Das R, Kumar BA (2022c) Monitoring the causes of pollution using groundwater quality and chemistry before and after the monsoon. Physics and Chemistry of the Earth, Parts A/B/C 103228
Rashid A, Guan D-X, Farooqi A, Khan S, Zahir S, Jehan S, Khattak SA, Khan MS, Khan R (2018) Fluoride prevalence in groundwater around a fluorite mining area in the flood plain of the River Swat, Pakistan. Sci Total Environ 635:203–215
Rashid A, Farooqi A, Gao X, Zahir S, Noor S, Khattak JA (2020) Geochemical modeling, source apportionment, health risk exposure and control of higher fluoride in groundwater of sub-district Dargai, Pakistan. Chemosphere 243:125409
Rashid A, Ayub M, Khan S, Ullah Z, Ali L, Gao X, Li C, El-Serehy HA, Kaushik P, Rasool A (2022) Hydrogeochemical assessment of carcinogenic and non-carcinogenic health risks of potentially toxic elements in aquifers of the Hindukush ranges, Pakistan: insights from groundwater pollution indexing, GIS-based, and multivariate statistical approaches. Environ Sci Pollut Res 29:75744–75768
Rasool A, Farooqi A, Xiao T, Ali W, Noor S, Abiola O, Ali S, Nasim W (2018) A review of global outlook on fluoride contamination in groundwater with prominence on the Pakistan current situation. Environ Geochem Health 40:1265–1281
Ravindra B, Subba Rao N, Dhanamjaya Rao E (2022) Groundwater quality monitoring for assessment of pollution levels and potability using WPI and WQI methods from a part of Guntur district, Andhra Pradesh, India. Environ Dev Sustain 1–31
Raza M, Farooqi A, Niazi NK, Ahmad A (2016) Geochemical control on spatial variability of fluoride concentrations in groundwater from rural areas of Gujrat in Punjab, Pakistan. Environ Earth Sci 75:1–16
Rehman JU, Ahmad N, Ullah N, Alam I, Ullah H (2020) Health risks in different age group of nitrate in spring water used for drinking in Harnai, Balochistan, Pakistan. Ecol Food Nutr 59:462–471
Rezaei M, Nikbakht M, Shakeri A (2017) Geochemistry and sources of fluoride and nitrate contamination of groundwater in Lar area, south Iran. Environ Sci Pollut Res 24:15471–15487
Sahin R, Kumar A, Chandrakar R, Michalska-Domańska M, Dubey V (2021) 3 The physico-chemical interaction of fluorine with the environment. Water Resource Technology: Management for Engineering Applications 17
Sajjad MM, Wang J, Abbas H, Ullah I, Khan R, Ali F (2022) Impact of climate and land-use change on groundwater resources, study of Faisalabad District, Pakistan. Atmosphere 13:1097
Sakram G, Kuntamalla S, Machender G, Dhakate R, Narsimha A (2019) Multivariate statistical approach for the assessment of fluoride and nitrate concentration in groundwater from Zaheerabad area, Telangana State, India. Sustain Water Resources Manag 5:785–796
Schoeller H (1965) Qualitative evaluation of groundwater resources. Methods and techniques of groundwater investigations and development, vol 5483. UNESCO, Paris, France
Selvam S, Venkatramanan S, Hossain M, Chung S, Khatibi R, Nadiri A (2020) A study of health risk from accumulation of metals in commercial edible fish species at Tuticorin coasts of southern India. Estuar Coast Shelf Sci 245:106929
Shukla S, Saxena A (2018) Global status of nitrate contamination in groundwater: its occurrence, health impacts, and mitigation measures. In: Handbook of environmental materials management, pp 869–888
Singh G, Rishi MS, Herojeet R, Kaur L, Sharma K (2020) Evaluation of groundwater quality and human health risks from fluoride and nitrate in semi-arid region of northern India. Environ Geochem Health 42:1833–1862
Soomro F, Rafique T, Michalski G, Azhar Ali S, Naseem S, Khan MU (2017) Occurrence and delineation of high nitrate contamination in the groundwater of Mithi sub-district, Thar Desert, Pakistan. Environ Earth Sci 76:1–9
Su C, Wang Y, Xie X, Li J (2013) Aqueous geochemistry of high-fluoride groundwater in Datong Basin, Northern China. J Geochem Explor 135:79–92
Su C, Wang Y, Xie X, Zhu Y (2015) An isotope hydrochemical approach to understand fluoride release into groundwaters of the Datong Basin Northern China. Environ Sci: Processes & Impacts. 17:791–801
Su C, Zhu Y, Abbas Z, Huq M (2016) Sources and controls for elevated arsenic concentrations in groundwater of Datong Basin, northern China. Environ Earth Sci 75:1–13
Su H, Kang W, Li Y, Li Z (2021) Fluoride and nitrate contamination of groundwater in the Loess Plateau, China: sources and related human health risks. Environ Pollut 286:117287
Subba Rao N (2021) Spatial distribution of quality of groundwater and probabilistic non-carcinogenic risk from a rural dry climatic region of South India. Environ Geochem Health 43:971–993
Subba Rao N, Ravindra B, Wu J (2020) Geochemical and health risk evaluation of fluoride rich groundwater in Sattenapalle Region, Guntur district, Andhra Pradesh, India. Hum Ecol Risk Assess Int J 26:2316–2348
Swarzenski H (1965) A Frankish Faience Madonna. Bullet Museum Fine Arts 63:183–195
Tahir MA, Rasheed H (2008) Distribution of nitrate in the water resources of Pakistan. Afr J Environ Sci Technol 2:397–403
Talib MA, Tang Z, Shahab A, Siddique J, Faheem M, Fatima M (2019) Hydrogeochemical characterization and suitability assessment of groundwater: a case study in Central Sindh, Pakistan. Int J Environ Res Public Health 16:886
Talpur SA, Noonari TM, Rashid A, Ahmed A, Jat Baloch MY, Talpur HA, Soomro MH (2020) Hydrogeochemical signatures and suitability assessment of groundwater with elevated fluoride in unconfined aquifers Badin district Sindh, Pakistan. SN Appl Sci 2:1–15
Tariq A, Mumtaz F, Zeng X, Baloch MYJ, Moazzam MF, Environment, (2022) Spatio-temporal variation of seasonal heat islands mapping of Pakistan during 2000–2019, using day-time and night-time land surface temperatures MODIS and meteorological stations data. Remote Sens Applic: Soc Environ 27:100779
Tran DA, Tsujimura M, Loc HH, Dang DH, Le Vo P, Ha DT, Trang NTT, Thuc PTB, Dang TD, Batdelger O (2021) Groundwater quality evaluation and health risk assessment in coastal lowland areas of the Mekong Delta, Vietnam. Groundw Sustain Dev 15:100679
Uddin M, Chow C, Su S (2018) Classification methods to detect sleep apnea in adults based on respiratory and oximetry signals: a systematic review. Physiol Meas 39:03TR01
Ullah R, Malik RN, Qadir A (2009) Assessment of groundwater contamination in an industrial city, Sialkot, Pakistan. Afr J Environ Sci Technol 3
Ullah Z, Rashid A, Ghani J, Nawab J, Zeng X-C, Shah M, Alrefaei AF, Kamel M, Aleya L, Abdel-Daim MM (2022) Groundwater contamination through potentially harmful metals and its implications in groundwater management. Front Environ Sci 10:2077

USEPA (2005) Guidelines for carcinogen risk assessment. In Risk assessment forum; EPA/630/P-03 F. US Environmental Protection Agency, Washington, DC

Wang Z, Guo H, Xing S, Liu H (2021) Hydrogeochemical and geothermal controls on the formation of high fluoride groundwater. J Hydrol 598:126372

Ward MH, Jones RR, Brender JD, De Kok TM, Weyer PJ, Nolan BT, Villanueva CM, Van Breda SG (2018) Drinking water nitrate and human health: an updated review. Int J Environ Res Public Health 15:1557

Water Environmental Federation; APHA Association (2005) Standard methods for the examination of water and wastewater. American Public Health Association, Washington, DC, 21 p

WHO (2022) *Guidelines for drinking-water quality: incorporating the first and second addenda*. WHO, Geneva

Xiao Y, Liu K, Hao Q, Li Y, Xiao D, Zhang Y (2022a) Occurrence, controlling factors and health hazards of fluoride-enriched groundwater in the lower flood plain of Yellow River, Northern China. Exposure and Health 1–14

Xiao Y, Liu K, Hao Q, Xiao D, Zhu Y, Yin S, Zhang Y (2022b) Hydrogeochemical insights into the signatures, genesis and sustainable perspective of nitrate enriched groundwater in the piedmont of Hutuo watershed, China. Catena 212:106020

Xu P, Bian J, Li Y, Wu J, Sun X, Wang Y (2022) Characteristics of fluoride migration and enrichment in groundwater under the influence of natural background and anthropogenic activities. Environ Pollut 314:120208

Xue-Jie G, Mei-Li W, Giorgi F (2013) Climate change over China in the 21st century as simulated by BCC_CSM1. 1-RegCM4. 0. Atmos Ocean Sci Lett 6:381–386

Yadav KK, Gupta N, Kumar V, Choudhary P, Khan SA (2018) GIS-based evaluation of groundwater geochemistry and statistical determination of the fate of contaminants in shallow aquifers from different functional areas of Agra city, India: levels and spatial distributions. RSC Adv 8:15876–15889

Yan J, Chen J, Zhang W, Ma F (2020) Determining fluoride distribution and influencing factors in groundwater in Songyuan, Northeast China, using hydrochemical and isotopic methods. J Geochem Explor 217:106605

Younas A, Mushtaq N, Khattak JA, Javed T, Rehman HU, Farooqi A (2019) High levels of fluoride contamination in groundwater of the semi-arid alluvial aquifers, Pakistan: evaluating the recharge sources and geochemical identification via stable isotopes and other major elemental data. Environ Sci Pollut Res 26:35728–35741

Yousefi M, Ghoochani M, Mahvi AH (2018) Health risk assessment to fluoride in drinking water of rural residents living in the Poldasht city, northwest of Iran. Ecotoxicol Environ Saf 148:426–430

Zhang H, Selim H (2005) Kinetics of arsenate adsorption−desorption in soils. Environ Sci Technol 39:6101–6108

Zhang Y, Wu J, Xu B (2018) Human health risk assessment of groundwater nitrogen pollution in Jinghui canal irrigation area of the loess region, northwest China. Environ Earth Sci 77:1–12

Zhang W, Chai J, Li S, Wang X, Wu S, Liang Z, Baloch MYJ, Silva LF, Zhang D (2022a) Physiological characteristics, geochemical properties and hydrological variables influencing pathogen migration in subsurface system: what we know or not? Geosci Front 13(6):101346

Zhang W, Zhu Y, Gu R, Liang Z, Xu W, Jat Baloch MY (2022b) Health risk assessment during in situ remediation of Cr (VI)-contaminated groundwater by permeable reactive barriers: a field-scale study. Int J Environ Res Public Health 19:13079

Zhou Y, Li P, Chen M, Dong Z, Lu C (2021) Groundwater quality for potable and irrigation uses and associated health risk in southern part of Gu'an County, North China Plain. Environ Geochem Health 43:813–835

Terms and Conditions

Springer Nature journal content, brought to you courtesy of Springer Nature Customer Service Center GmbH (“Springer Nature”).
Springer Nature supports a reasonable amount of sharing of research papers by authors, subscribers and authorised users (“Users”), for small-scale personal, non-commercial use provided that all copyright, trade and service marks and other proprietary notices are maintained. By accessing, sharing, receiving or otherwise using the Springer Nature journal content you agree to these terms of use (“Terms”). For these purposes, Springer Nature considers academic use (by researchers and students) to be non-commercial.
These Terms are supplementary and will apply in addition to any applicable website terms and conditions, a relevant site licence or a personal subscription. These Terms will prevail over any conflict or ambiguity with regards to the relevant terms, a site licence or a personal subscription (to the extent of the conflict or ambiguity only). For Creative Commons-licensed articles, the terms of the Creative Commons license used will apply.
We collect and use personal data to provide access to the Springer Nature journal content. We may also use these personal data internally within ResearchGate and Springer Nature and as agreed share it, in an anonymised way, for purposes of tracking, analysis and reporting. We will not otherwise disclose your personal data outside the ResearchGate or the Springer Nature group of companies unless we have your permission as detailed in the Privacy Policy.
While Users may use the Springer Nature journal content for small scale, personal non-commercial use, it is important to note that Users may not:

1. use such content for the purpose of providing other users with access on a regular or large scale basis or as a means to circumvent access control;
2. use such content where to do so would be considered a criminal or statutory offence in any jurisdiction, or gives rise to civil liability, or is otherwise unlawful;
3. falsely or misleadingly imply or suggest endorsement, approval , sponsorship, or association unless explicitly agreed to by Springer Nature in writing;
4. use bots or other automated methods to access the content or redirect messages
5. override any security feature or exclusionary protocol; or
6. share the content in order to create substitute for Springer Nature products or services or a systematic database of Springer Nature journal content.

In line with the restriction against commercial use, Springer Nature does not permit the creation of a product or service that creates revenue, royalties, rent or income from our content or its inclusion as part of a paid for service or for other commercial gain. Springer Nature journal content cannot be used for inter-library loans and librarians may not upload Springer Nature journal content on a large scale into their, or any other, institutional repository.
These terms of use are reviewed regularly and may be amended at any time. Springer Nature is not obligated to publish any information or content on this website and may remove it or features or functionality at our sole discretion, at any time with or without notice. Springer Nature may revoke this licence to you at any time and remove access to any copies of the Springer Nature journal content which have been saved.
To the fullest extent permitted by law, Springer Nature makes no warranties, representations or guarantees to Users, either express or implied with respect to the Springer nature journal content and all parties disclaim and waive any implied warranties or warranties imposed by law, including merchantability or fitness for any particular purpose.
Please note that these rights do not automatically extend to content, data or other material published by Springer Nature that may be licensed from third parties.
If you would like to use or distribute our Springer Nature journal content to a wider audience or on a regular basis or in any other manner not expressly permitted by these Terms, please contact Springer Nature at

onlineservice@springernature.com